Proceedings of Lunar and Planetary Science, Volume 22, pp. 275-301
Lunar and Planetary Institute, Houston, 1992

Compositional Variations in Apollo 17 Soils and Their Relationship to the Geology of the Taurus-Littrow Site

Randy L. Korotev* **and Daniel T. Kremser**

Department of Earth and Planetary Sciences, Washington University, St. Louis MO 63130

New compositional data for major and trace elements in Apollo 17 soils are combined with literature data to constrain a mass-balance model that accounts for the compositions of most soils as mixtures of a small number of lithologic components observed at the site. These components include high-Ti mare basalt, very-low-Ti (VLT) mare basalt, orange pyroclastic glass, noritic breccia, anorthositic norite, and a meteoritic component. Soils from the area of the North Massif require an additional component with a high Mg/Fe ratio; this component can be modeled as a mixture of troctolite and norite similar to plutonic rocks found at the North Massif (e.g., troctolite 76535 and norite 78255). No high-Mg/Fe component is required for soils from the South Massif, but soils from station 2 (only) on the South Massif are modeled better when a 4% component of KREEP basalt (such as found in station 2 breccia 72275) is included. For soils from the valley floor the model predicts that approximately 8% of the basalt component is VLT basalt and that they contain 10-25% pyroclastic orange-glass component. The abundance of orange-glass component required for mass balance is less for most soils than estimated from previous models, but model abundances obtained here agree better with abundances obtained in petrographic studies. Only 6% orange-glass component is required for mass balance in the gray soil from station 4 (samples 74241 and 74261), which was collected from the same trench as a concentrated deposit of orange glass (74220). The highland material in the gray soil (station 4) and in soils from the center of the valley floor (stations LM, 1, LRV-12) has a high proportion of noritic breccia component; this material is probably old regolith excavated from beneath the valley floor, not regolith derived from impacts into the massifs. Sample 73131, which was collected as a regolith clod at station 2A on the South Massif but was disaggregated during its trip to Earth, is composed almost entirely of highland material; it is the only regolith sample from the Apollo 17 site that is virtually uncontaminated with mare-derived material. It has lower concentrations of Sc, Fe, and incompatible trace elements than any other South Massif soil and probably derives from the lower slope of the massif. The composition of ropy glass particles found in the gray soil from station 4 can be modeled well by the same model that accounts for Apollo 17 soils, thus the ropy glass is probably of local origin and is not ejecta from Tycho Crater. The inferred composition of the nonmare components of the ropy glass particles is nearly identical to that of regolith breccia 73131, suggesting that the ropy glass derives from an impact into the local highlands.

1. INTRODUCTION

The Apollo 17 mission to the Moon landed in the Taurus-Littrow valley on the edge of Mare Serenitatis in December 1972. The Taurus-Littrow valley floor is covered with mare basalt and the surrounding massifs are composed of ejecta deposited by the impact that excavated the basin of Mare Serenitatis (Fig. 1) (*Wolfe et al.*, 1981). The site was selected so that material from both the highland massifs and the basalt-filled valley could be sampled, and rocks of both affinities were obtained. Astronauts Eugene A. Cernan and Harrison H. Schmitt also collected a large number of regolith samples. These include samples from the surface and from trenches using scoops, and from depth using coring equipment.

Because the astronauts collected samples on traverses of more than 31 km in length, starting on the mafic maria and ranging into the surrounding feldspathic highlands, the soil (regolith fines) samples span a large range of chemical composition. *Rhodes et al.* (1974) showed that the compositional variations were related in a reasonable way to the geology and geography of the site (Fig. 2) and that the variations resulted from differences in the proportions of four lithologic components. These components represented (1) high-Ti mare basalt (the predominant rock type of the valley floor), (2) orange glass (sample 74220, which consisted almost entirely of orange and devitrified black pyroclastic glass beads), (3) "noritic breccia" (typical melt matrix of massif-derived boulders), and (4) "anorthositic gabbro" (a typical clast composition in the breccia boulders). Three compositional groups were recognized among the soils: (1) valley-floor-type soils, dominated by mare basalt and orange glass but containing some materials from the surrounding highlands, (2) South Massif-type soils consisting primarily of about equal proportions of noritic breccia and anorthositic gabbro with only minor (usually <10%) contamination by mare materials, and (3) North Massif-type soils, which contained a 2:1 ratio of anorthositic gabbro to noritic breccia and a large component (>25%) of mare material (basalt and orange glass).

Since 1974, a number of lithologies not represented by the four model components of *Rhodes et al.* (1974) have been discovered among the Apollo 17 samples. These include very-low-Ti (VLT) mare basalt, a primitive variant of high-Ti mare basalt, KREEP basalt, and plutonic highland rocks such as norite, troctolite, dunite, and anorthosite (*Blanchard et al.*, 1975; *Dymek et al.*, 1975; *Winzer et al.*, 1975; *Taylor et al.*, 1977; *Vaniman and Papike*, 1977a; *Warren and Wasson*,

* Also at McDonnell Center for the Space Sciences, Washington University, St. Louis MO 63130

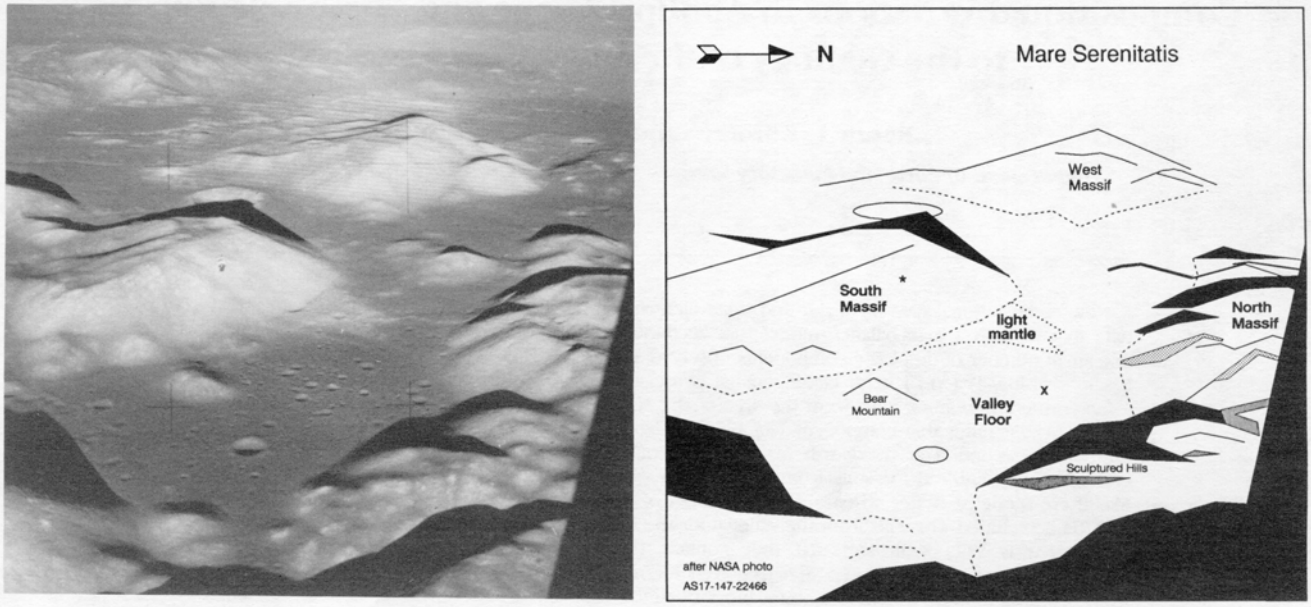

Fig. 1. View of Taurus-Littrow valley as photographed from the lunar module (LM). The valley is about 7 km wide. The X in the sketch marks the landing point of the LM. The South Massif is over 2 km high. The light mantle is an avalanche deposit formed when secondaries from the Tycho event impacted the upper slopes of the South Massif (*Lucchitta,* 1977). The orbiting command module can be seen in the photograph with the South Massif in the background (location marked by asterisk in the sketch). Figure and data are based on Fig. 2 of *Wolfe et al.* (1981). (NASA photograph AS17-147-22466.)

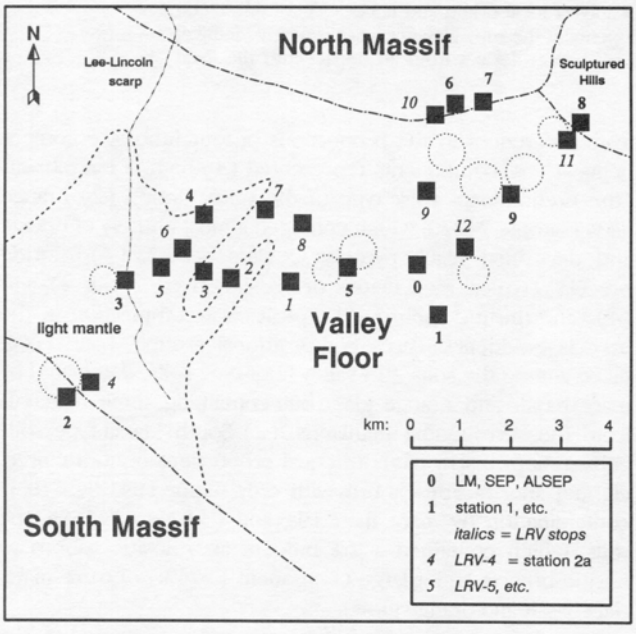

Fig. 2. Schematic map of the Apollo 17 landing site with location of sample stations and lunar roving vehicle (LRV) stops. Sample station numbers are indicated with bold numerals (**0** through **9**, with **0** representing station LM/ALSEP) and LRV stops with italic numerals (*1* through *12*). The same scheme is used in subsequent figures. Based on Fig. 7 of *Wolfe et al.* (1981).

1978, 1979; *Wentworth et al.,* 1979; *Salpas et al.,* 1987, 1988; *Ryder,* 1990; *Warren et al.,* 1991). We undertook this study largely to assess, from a compositional standpoint, whether any of these lithologies are volumetrically significant in the soils and, if so, how their relative abundances relate to site geology.

Evaluation of this problem has been hampered by the lack of a self-consistent dataset for a sufficiently large number of samples and elements. Although 20 years have elapsed since the Apollo 17 mission, no compositional data have been reported for many of the 68 samples of surface and trench soils from Apollo 17 listed in the *Handbook of Lunar Soils* (*Morris et al.,* 1983). Only 38 have been analyzed for major-element concentrations by X-ray fluorescence (XRF), a high-precision technique, and less than half have been analyzed for trace elements by instrumental neutron activation analysis (INAA), a high-precision technique for many elements. To help fill the gaps in the database, we report here results of 77 analyses of 55 samples of <1-mm fines by INAA, including all samples of surface and trench soils not previously studied by INAA. We also report results of 39 analyses of 37 samples for major elements by electron microprobe analysis of fused beads (FB-EMPA). In addition, we report major- and trace-element data for some ropy glass particles from station 4 and consider their origin.

2. SAMPLES AND ANALYSIS

Most of the data presented here are based on allocations of 100-mg (nominal) subsamples from <1-mm grain-size fractions prepared by NASA shortly after the mission (i.e., samples

designated 7XXX1). In three cases (samples 72150, 74220, and 78250) the allocated subsamples consisted of unsieved material (i.e., 7XXX0), but in each of these cases the subsamples contained no >1-mm particles. For most of the samples a single 50-mg split (i.e., half the allocated subsample) was used for INAA, but for 22 samples both 50-mg splits were analyzed, exhausting the allocation. The two splits are designated A and B in Tables A1 and A2. For 37 samples, 50-mg splits were ground by hand with an aluminum oxide mortar and pestle under acetone; approximately 10-mg portions of these powders were fused for major-element analysis (below). For most of these samples, the ground split was the half remaining after the INAA split was taken, but for those samples analyzed in duplicate by INAA, the neutron-irradiated splits were ground and fused after radioassay. For two samples (74241 and regolith breccia sample 73131), both duplicate splits analyzed by INAA were fused, resulting in a total of 39 analyses of major elements for 37 samples of <1-mm fines. No sample analyzed by INAA was ground prior to neutron irradiation.

In addition, six individual ropy glass particles (1.3 to 7 mg each) from sample 74242 (the 1-2-mm grain-size fraction of 74240) were analyzed by INAA. After INAA, the six particles were combined, ground together, and fused for major-element analysis by FB-EMPA.

INAA was done using the methods of *Korotev* (1991). Powders were fused for major-element analysis on a Mo strip heater (*Brown,* 1977) under Ar at atmospheric pressure. Concentrations of SiO_2, TiO_2, Al_2O_3, FeO, MgO, and CaO were determined by electron microprobe using the mean results for three 10-μm spots per glass bead; standard techniques were used for data reduction (*Bence and Albee,* 1968). Based on previous XRF analyses, the sum of these six oxides typically accounts for 98.6% of the mass of Apollo 17 soils; the remaining 1.4% is primarily MnO, Na_2O, K_2O, Cr_2O_3, P_2O_5, and S (*Rhodes et al.,* 1974; *Rose et al.,* 1974; *Duncan et al.,* 1974). (We did not determine concentrations for these elements by EMPA because Na and Cr were determined precisely by INAA and because MnO, K_2O, and P_2O_5 correlate strongly with elements determined by INAA and thus provide no unique constraint on the model to be presented.) Based on our raw FB-EMPA analyses, oxide concentrations for the six analyzed elements typically summed to around 97-98% and were occasionally as low as 95%, because of Mo oxide dissolved in the glass or Mo metal, which was observed as micrometer-sized blebs in some of the prepared glasses. Thus, results for each spot were normalized so that the concentrations of the six analyzed elements summed to 98.60%.

Thirteen of the samples analyzed by FB-EMPA have been previously analyzed by XRF. Concentrations we obtained for four of the six elements (SiO_2, FeO, MgO, and CaO) differed systematically from those of the previous studies for these samples. Differences for MgO and CaO were the greatest, with FB-EMPA/XRF ratios averaging 1.026 ± 0.010 for MgO and 0.975 ± 0.006 for CaO (Table 1, column 1). We do not know the cause of these discrepancies. National Bureau of Standards glass K-411 was used as the standard for each of the four elements (*Marinenko,* 1982) (other glasses were used for TiO_2 and Al_2O_3). However, results obtained for other standards run concurrently (e.g., glass K-412) did not indicate any systematic error. Subsequent tests on a terrestrial sample show that including Mo in the analysis does not affect the results for MgO and CaO by as much as 2.5%. Thus, in order to obtain a dataset consistent with previous work, we normalized the concentrations of all elements obtained by FB-EMPA a second time by dividing by the ratios of column 1a of Table 1. This yielded new sums for the six analyzed oxides of 98.5%, insignificantly different from the value used for the first normalization. We judge the precision of the final FB-EMPA results (Table A2) to be good; for the 13 samples analyzed by both techniques, differences in percent oxide determined by FB-EMPA and those obtained by XRF on the same sample (although on different splits) was typically on the order of a few percent of the value (Table 1, column 2c).

TABLE 1. Comparison of concentrations obtained by FB-EMPA (this study) with those obtained by XRF (literature data) for 13 samples analyzed in common (XRF data from *Rhodes et al.,* 1974; *Rose et al.,* 1974; *Duncan et al.,* 1974).

	Before Norm. (Ratio)		After Norm. (Difference)		
Column:	FB/XRF (1a)	±95% (1b)	s (2a)	conc. (2b)	s/conc. (2c)
SiO_2	1.012	0.005	0.43	42.1	0.010
TiO_2	1.004	0.019	0.35	6.2	0.056
Al_2O_3	0.993	0.018	0.33	14.7	0.022
FeO	0.989	0.014	0.47	14.1	0.033
MgO	1.026	0.010	0.19	9.9	0.019
CaO	0.975	0.006	0.15	11.5	0.013

(1a) Mean ratio of FB-EMPA to XRF concentrations. (FB-EMPA data after first normalization to sum to 98.6%, but before second normalization; see text.)
(1b) Uncertainty on values of column 1a, 95% confidence limit (n = 13).
(2a) Sample standard deviation in differences between FB-EMPA and XRF concentrations [i.e., percent oxide by FB-EMPA (after second normalization by values of column 1a) minus percent oxide by XRF].
(2b) Average concentration (percent oxide) of the 13 samples.
(2c) Relative standard deviation (column 2a divided by column 2b). The high value for FeO is probably caused by nonuniform distribution of metallic Fe grains, not by analytical imprecision. The high value for TiO_2 reduces to 0.032 if sample 74241A is excluded (Table A1).

3. RESULTS

3.1. <1-mm Fines

Soil compositions at Apollo 17 vary substantially from station to station. Concentrations of Sc and TiO_2 are up to 5 and 7 times greater, respectively, in valley-floor soils than in soils from the light mantle near the South Massif. Lanthanum concentrations vary by more than a factor of three among the samples (INAA results, Table A1; FB-EMPA results, Table A2). Because most soils from a given sampling station are similar to each other in composition (section 3.1.2), station-average compositions for both major and trace elements are presented in Table 2. Data for some compositionally unique soil samples (e.g., 74220) and stations where only one sample was taken

TABLE 2. Average compositions by station of Apollo 17 surface and trench soils (stations arranged in approximate order of decreasing FeO concentration).

Station:		4	5	5	1	LRV-12	LM/ALSEP	LRV-1	LRV-7	LRV-8	4	9	LRV-3
Sample:		orange	75061	75081	mean	mean	mean	72131	75111	75121	gray	mean	mean
SiO_2	%	38.6	39.5	40.1	39.9	39.9	40.8	41.3	41.8	41.9	41.5	42.1	42.2
TiO_2	%	8.76	10.4	9.41	9.63	9.97	8.47	7.95	6.83	6.58	7.74	6.39	5.49
Al_2O_3	%	6.53	10.5	11.25	10.85	11.15	12.1	12.6	12.8	13.45	13.3	13.9	14.35
FeO	%	22.2	18.0	17.4	17.75	17.35	16.6	16.3	16.1	15.7	15.5	15.35	14.75
MgO	%	14.39	9.59	9.51	9.64	9.36	9.76	9.41	10.25	9.86	9.31	9.98	10.42
MnO	%	0.29	0.25	0.25	0.24	n.d.	0.23	n.d.	n.d.	n.d.	0.21	0.20	0.22
CaO	%	7.69	10.7	10.9	10.75	10.75	11.1	11.15	10.7	11.25	11.35	11.25	11.25
Na_2O	%	0.366	0.354	0.373	0.391	0.376	0.392	0.396	0.419	0.398	0.470	0.410	0.398
K_2O	%	0.08	0.08	0.08	0.08	n.d.	0.08	n.d.	n.d.	n.d.	0.12	0.10	0.11
P_2O_5	%	0.04	0.06	0.07	0.07	n.d.	0.08	n.d.	n.d.	n.d.	0.095	0.075	0.08
S	%	0.07	0.13	0.12	0.13	n.d.	0.12	n.d.	n.d.	n.d.	0.12	0.12	0.08
Cr_2O_3	%	0.68	0.51	0.43	0.46	0.46	0.44	0.43	0.45	0.42	0.42	0.41	0.42
Sc	μg/g	48.3	72.6	66.4	66.1	66.3	60.2	58.4	49.3	49.9	56.5	50.1	42.3
Cr	μg/g	4650	3380	3220	3180	3150	3030	2960	3060	2900	2870	2830	2860
Co	μg/g	61.5	27.0	30.6	32.0	31.2	34.2	33.4	38.3	38.2	28.4	36.8	42.8
Ni*	μg/g	113	60†	100	115	125	170	180	160	220	120	230	285
Zn	μg/g	273	19	33	57	n.d.	35	n.d.	n.d.	n.d.	70	30	58
Rb	μg/g	1.2	1.3	1.1	1.1	n.d.	1.3	n.d.	n.d.	n.d.	2.1	1.8	2.0
Sr	μg/g	205	162	164	166	175	168	150	200	210	154	147	168
Y	μg/g	46	87	75	74	n.d.	74	n.d.	n.d.	n.d.	78	62	55
Zr	μg/g	184	289	220	215	270	229	180	220	n.d.	266	197	200
Nb	μg/g	14	21	20	19	n.d.	21	n.d.	n.d.	n.d.	22	18	16
Ba	μg/g	78	92	104	105	95	98	96	123	124	121	103	124
La	μg/g	5.94	6.87	7.96	7.43	7.16	8.03	8.18	8.96	9.07	9.60	8.68	9.63
Ce	μg/g	18.1	21.2	24.2	22.8	22.4	23.8	24.3	26.2	26.6	28.1	25.2	27.7
Nd	μg/g	16.6	20.0	22.0	17.9	17.5	21.8	21.0	19.8	17.0	20.0	19.0	21.0
Sm	μg/g	6.71	8.43	8.78	8.24	7.96	8.11	7.76	7.56	7.84	8.55	7.26	7.10
Eu	μg/g	1.79	1.69	1.72	1.71	1.66	1.72	1.62	1.56	1.59	1.62	1.53	1.44
Tb	μg/g	1.48	2.14	2.16	2.07	1.97	1.99	1.85	1.71	1.82	2.03	1.76	1.64
Yb	μg/g	4.31	8.08	8.04	7.47	7.32	7.17	6.65	5.98	6.41	7.30	6.86	5.67
Lu	μg/g	0.590	1.12	1.11	1.04	1.04	0.993	0.920	0.860	0.922	1.03	0.989	0.802
Hf	μg/g	5.77	7.65	7.73	7.26	7.24	6.84	6.60	6.17	6.65	7.19	13.98	5.99
Ta	μg/g	1.00	1.40	1.36	1.32	1.28	1.18	1.20	1.01	1.06	1.20	1.03	0.91
Ir*	ng/g	0.7	2.5	5.7	5.5	6.0	4.8	5.0	6.3	12.0	4.1	8.4	10.8
Au*	ng/g	0.3	1.5	2.1	2.3	1.0	3.6	5.9	2.1	4.7	2.8	3.6	4.8
Th	μg/g	0.42	0.58	0.78	0.72	0.68	0.88	0.93	1.20	1.10	1.11	1.15	1.31
U	μg/g	0.13	0.15	0.2	0.22	0.10	0.31	0.36	0.29	0.53	0.28	0.40	0.39

[usually lunar roving vehicle (LRV) stops] are tabulated separately. For completeness, the data in Table 2 include literature data for samples and some elements not analyzed for this study.

The three groupings of soil compositions recognized by *Rhodes et al.* (1974) are evident in Figs. 3 and 4. Soils from the valley floor have the highest concentrations of Fe and Sc because they are composed largely of mare basalt. Soils derived from the South Massif (i.e., those collected on the light mantle deposit) are the least "contaminated" with mare basalt and have the greatest proportion of KREEP-bearing, noritic impact-melt breccia (Fig. 5). As a result, they have the lowest concentrations of Sc and Fe and the highest concentrations of incompatible trace elements (ITEs) such as Sm and La, as well as high concentrations of Na. Soils from the North Massif contain somewhat more mare material than South Massif soils and have the largest proportions of ITE-poor "anorthositic gabbro," thus they have greater Sc and Fe concentrations than the South Massif soils and the lowest concentrations of most ITEs. All other soils are intermediate in composition to these three extremes except those from station 4. "Soil" 74220 from station 4 at Shorty Crater consists almost entirely of orange and black pyroclastic glass beads (*Heiken and McKay,* 1974) and is compositionally unique. The other two station 4 soils, 74241 (two splits plotted in Figs. 3 and 4) and 74261 (one split), are unusual in that they are gray in color and have a low abundance of agglutinates (*Heiken and McKay,* 1974). They are compositionally distinct from all other soils and considerably different in composition from 74220. In particular, they contain higher concentrations of Na than other similarly mafic soils (Fig. 4). [All information about sample and station locations reported here is derived from *Wolfe et al.* (1981)].

3.1.1. LRV stops. While traveling from one sampling station to another in the LRV the astronauts sometimes stopped to collect rocks and one or two soil samples. Soils from LRV stops (coded as italic numerals in the figures) are usually similar in composition to soils from nearby sampling stations. For example, the LRV-11 soil (78121) is indistinguishable from nearby station 8 soils, and the two LRV-12 soils (70311 and 70321) are most similar to soils from station 1 (Figs. 3 and 4). Soils from LRV-5 (74111) and LRV-6 (74121) on the light mantle are most similar to soils from nearby station 3; however, they are more distant from the massif and consequently more mafic (greater Fe and Sc concentrations). Other similarities are

TABLE 2. (continued).

Station:	LRV-9	LRV-2	LRV-11	8	7	LRV-10	6	LRV-6	LRV-5	3	2	2A	2A/LRV-4
Sample:	76121	72141	78121	mean	mean	76131	mean	74121	74111	mean	mean	mean	73131 RB
SiO_2	42.2	43.1	43.2	43.4	43.7	43.5	43.5	44.5	44.8	44.9	45.0	45.0	45.0
TiO_2	6.14	4.37	4.50	4.30	3.88	3.74	3.35	2.56	2.56	1.80	1.50	1.32	0.92
Al_2O_3	14.25	16.1	16.25	16.6	17.25	17.5	18.25	19.35	19.9	20.35	20.7	21.3	22.55
FeO	14.6	13.40	12.69	12.29	11.59	11.18	10.73	10.29	9.75	8.72	8.72	8.34	7.13
MgO	9.83	10.25	10.02	10.21	10.08	10.51	10.76	9.93	8.91	10.18	9.93	9.87	9.36
MnO	n.d.	0.19	n.d.	0.17	0.17	n.d.	0.15	0.13	n.d.	0.11	0.12	0.12	n.d.
CaO	11.3	11.85	11.85	11.75	11.9	12.1	12.15	12.45	12.75	12.85	12.75	12.9	13.45
Na_2O	0.405	0.402	0.410	0.380	0.399	0.415	0.398	0.427	0.434	0.449	0.457	0.437	0.434
K_2O	n.d.	0.12	n.d.	0.09	0.11	n.d.	0.12	0.13	n.d.	0.16	0.165	0.15	n.d.
P_2O_5	n.d.	0.10	n.d.	0.09	0.08	n.d.	0.095	0.135	n.d.	0.145	0.15	0.13	n.d.
S	n.d.	0.09	n.d.	0.095	0.08	n.d.	0.07	0.08	n.d.	0.06	0.07	0.065	n.d.
Cr_2O_3	0.39	0.35	0.34	0.34	0.32	0.30	0.28	0.25	0.26	0.22	0.23	0.21	0.18
Sc	43.7	35.8	37.0	36.4	33.2	31.6	28.8	24.3	24.7	19.1	19.1	17.6	14.8
Cr	2640	2370	2360	2320	2160	2020	1920	1700	1780	1480	1580	1460	1260
Co	35.3	38.2	34.6	36.4	31.7	29.3	35.7	36.4	30.5	28.0	29.8	31.2	22.9
Ni*	230	230	310	245	250	200	275	325	240	240	265	275	190
Zn	n.d.	50	n.d.	31	31	n.d.	28	24	n.d.	20	20	17	n.d.
Rb	n.d.	2.3	n.d.	2.4	2.6	n.d.	2.7	3.6	n.d.	2.5	3.7	3.4	n.d.
Sr	140	155	150	165	145	190	155	151	178	140	158	153	146
Y	n.d.	53	n.d.	50	52	n.d.	48	54	n.d.	59	62	55	n.d.
Zr	230	186	250	186	200	230	183	240	250	220	271	229	200
Nb	n.d.	15	n.d.	14	15	n.d.	14	17	n.d.	11	16	14	n.d.
Ba	126	n.d.	107	115	132	144	129	n.d.	166	176	206	177	178
La	8.66	10.90	8.98	8.80	10.06	11.77	10.13	15.50	14.20	16.16	18.27	15.64	14.70
Ce	24.8	28.0	24.9	24.5	27.4	32.3	27.6	37.0	37.7	39.1	47.9	39.5	38.4
Nd	18.0	n.d.	17.0	18.3	18.5	23.0	19.7	n.d.	25.0	29.0	29.6	25.4	23.8
Sm	6.92	6.78	6.24	6.19	6.48	7.17	6.21	8.06	7.50	7.82	8.74	7.39	6.89
Eu	1.46	1.39	1.36	1.35	1.35	1.41	1.33	1.28	1.31	1.29	1.34	1.24	1.18
Tb	1.62	1.50	1.44	1.43	1.50	1.61	1.41	1.90	1.62	1.68	1.71	1.51	1.33
Yb	5.71	5.62	5.14	5.19	5.31	5.70	5.02	6.02	5.78	5.86	6.45	5.69	5.08
Lu	0.825	0.740	0.751	0.728	0.748	0.802	0.700	0.810	0.808	0.827	0.889	0.779	0.700
Hf	5.86	5.64	5.31	5.15	5.33	5.53	5.01	6.02	6.05	6.09	6.83	5.44	5.31
Ta	0.93	0.77	0.79	0.80	0.82	0.86	0.76	0.87	0.84	0.78	0.84	0.75	0.67
Ir*	7.0	25.	10.0	10.0	7.9	7.1	9.7	11.	8.0	10.2	8.4	11.8	5.8
Au*	1.6	10.	2.5	3.3	5.9	1.9	4.1	13.	2.3	5.6	3.5	4.9	2.6
Th	1.11	n.d.	1.32	1.34	1.57	1.87	1.63	2.60	2.40	3.03	3.19	2.54	2.53
U	0.25	0.30	0.32	0.35	0.42	0.52	0.44	n.d.	0.60	0.75	0.79	0.72	0.74

* Data for Ni and particularly Ir and Au are highly imprecise and not always representative, especially when based on only one sample.
† Estimated.

Sources of data: All data for MnO, K_2O, P_2O_5, S, Zn, Rb, Y, and Nb, and some data for SiO_2, TiO_2, Al_2O_3, FeO, MgO, CaO, Sr, and Zr are from *Duncan et al.* (1974), *Rhodes et al.* (1974), *Rose et al.* (1974); most data for stations 2A and 3 are from *Laul et al.* (1974) and *Wänke et al.* (1974); INAA data for 72141 (LRV-2) and 74121 (LRV-6) are from *Wänke et al.* (1974); all other data are from this work. n.d. = no data available.

not necessarily expected based on site geography. The composition of LRV-7 soil (75111) from the inner slope of the rim of Victory Crater at the edge of the light mantle deposit is very similar to that of station 9 soils, 7 km away (Fig. 2). Soil from LRV-8 (75121) is more similar in composition to soils from station 9 than to the soils from stations 5 and LRV-1, which are closer. The soils from station 2A (LRV-4) at the base of the South Massif are not as compositionally similar to soils from nearby station 2 as are the station 3 soils, further out on the light mantle.

3.1.2. Intrastation variability. Several soil samples were collected at each sampling station and these are generally more similar in composition to each other than they are to soils from other stations (Figs. 3 and 4). One obvious exception already noted is that orange-glass "soil" (74220) is distinctly different from the other station 4 soils (74241 and 74261), even though all were recovered from the same trench. At the Apollo 16 site, soils taken from trenches (e.g., 61221) or from the edges of craters (e.g., 60051) are often clearly different in composition from undisturbed surface soils collected at the same station; typically, the trench soils are compositionally more feldspathic (*Korotev,* 1981). Except for the station 4 trench, no similarly systematic differences occur among the Apollo 17 soils. For example, the station 9 soils span a narrow range of composition and Na, Eu, and ITE concentrations mutually correlate within this range (Fig. 4). Three of the five soils from station 9 (79221, 79441, and 79661) derive from different depths in a 17-cm-deep trench, but the compositional variations do not correlate with depth. Nearby drive tube 79001/2 also shows little compositional variation within this depth interval (*Morris et al.,* 1989). Similarly, four samples from station 8 represent different depths within a 25-cm-deep trench (78421, 78441, 78461, and 78481), yet they are all nearly identical in composition. However, the deepest sample (78421 from about 15-25 cm depth) has the highest concentrations of Sc and FeO and lowest

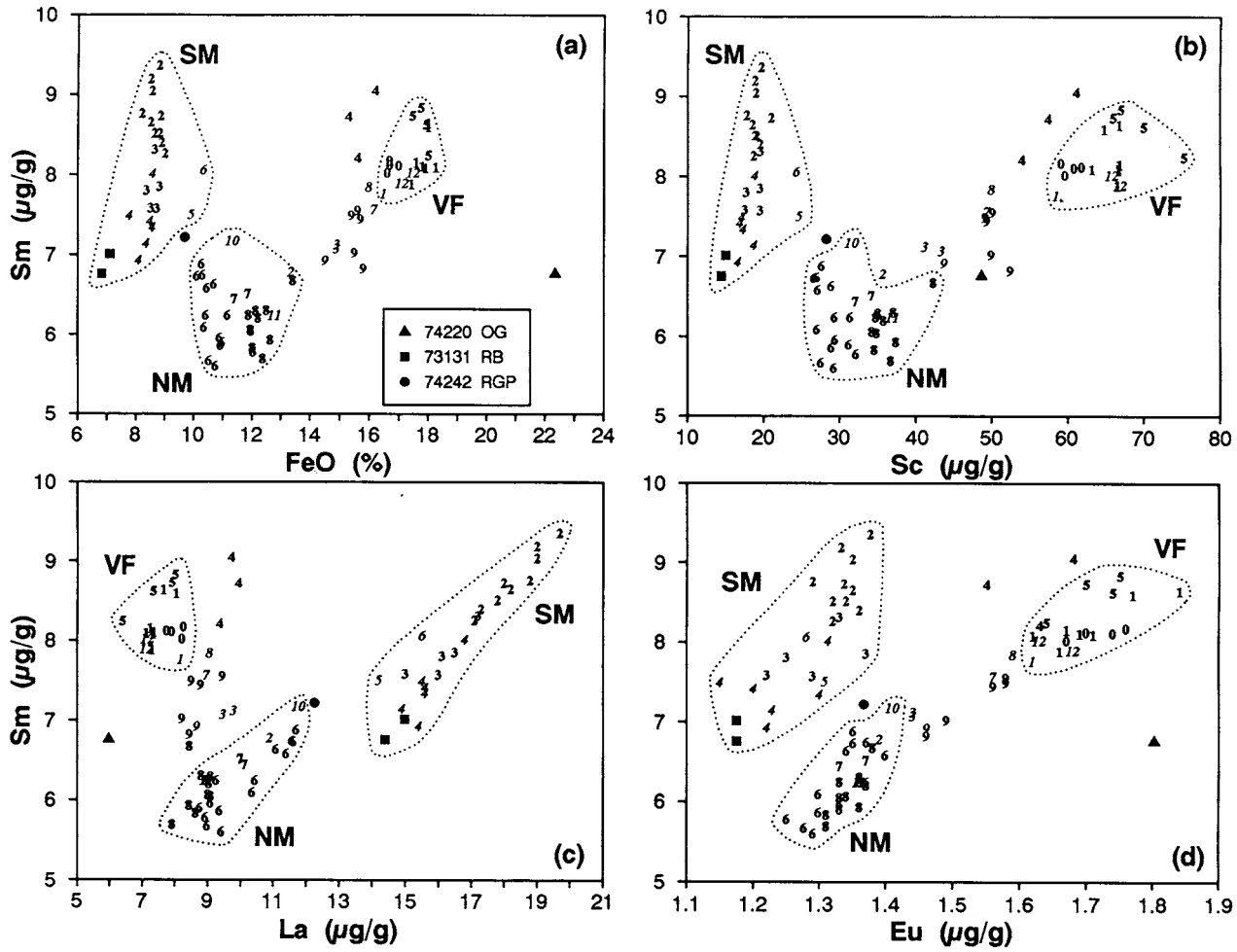

Fig. 3. Concentration of Sm plotted against concentrations of FeO, Sc, Eu, and La for Apollo 17 soils. For samples analyzed in duplicate, two points are plotted. The sample-station key is the same as in Fig. 2 (**bold** numerals equal sample station numbers, *italic* numerals = LRV stops, 4 = gray soils from station 4). Other symbols: SM = South Massif/light mantle soils, NM = North Massif soils, VF = valley-floor soils, OG = orange glass, RB = regolith breccia, and RGP = ropy glass particles. Data primarily from this work; some SM data from *Wänke et al.* (1974) and *Laul et al.* (1974). Because of the relative scaling of the axes, it appears that compositional variation among samples from a given station (e.g., stations 2 and 6) is greater for incompatible elements like Sm and La than for compatible elements like Sc and Fe; the relative variation is about the same, however (see Fig. 5).

concentration of La of the trench samples, suggesting a greater proportion of mare basalt. In terms of the model to be presented below, that proportion is ~30%, compared with 28% for the average of the other three soils.

The seven station 6 samples are similar to each other in composition. However, they appear to form two groups, with three samples having concentrations of Na, Sm, and other ITEs averaging about 1.03 times those of the other four (Fig. 4; Table A1). One of the high-ITE soils (76321) was collected on a boulder (block 1) and is believed to be ejecta from some nearby impact (*Wolfe et al.*, 1981). The second (76241) was collected in the shadow of a boulder (block 4) while the third (76261) is a surface sample collected a meter away. The four low-ITE soils were collected at greater distances from boulders (76031, 76221, and 76501) or below the surface (76281 was collected between 2 and 5 cm depth, just below 76261). As with the station 9 soils, Sm concentrations correlate with those of Na_2O (Fig. 4), suggesting that the enrichments are caused by a greater proportion of an ITE-rich lithology, probably noritic impact-melt breccia, in the three high-ITE soils.

Among the station 8 soils the single split of 78501 analyzed here is richer than the others in elements associated with mare basalt. It was collected on the rim of a small crater. The station 7 soils are intermediate, both compositionally and geographically, to the soils from stations 6 and 8 in the North Massif and Sculptured Hills area.

At the South Massif, the only systematic differences at station 2 are that the three samples collected as fillets from boulder 1 (72221, 72241, and 72261) have concentrations of ITEs about 1.06 times those of the other station 2 soils. The single station 3 sample analyzed here, 73211, falls within the compositional range of the station 2 soils, but has ITE concentra-

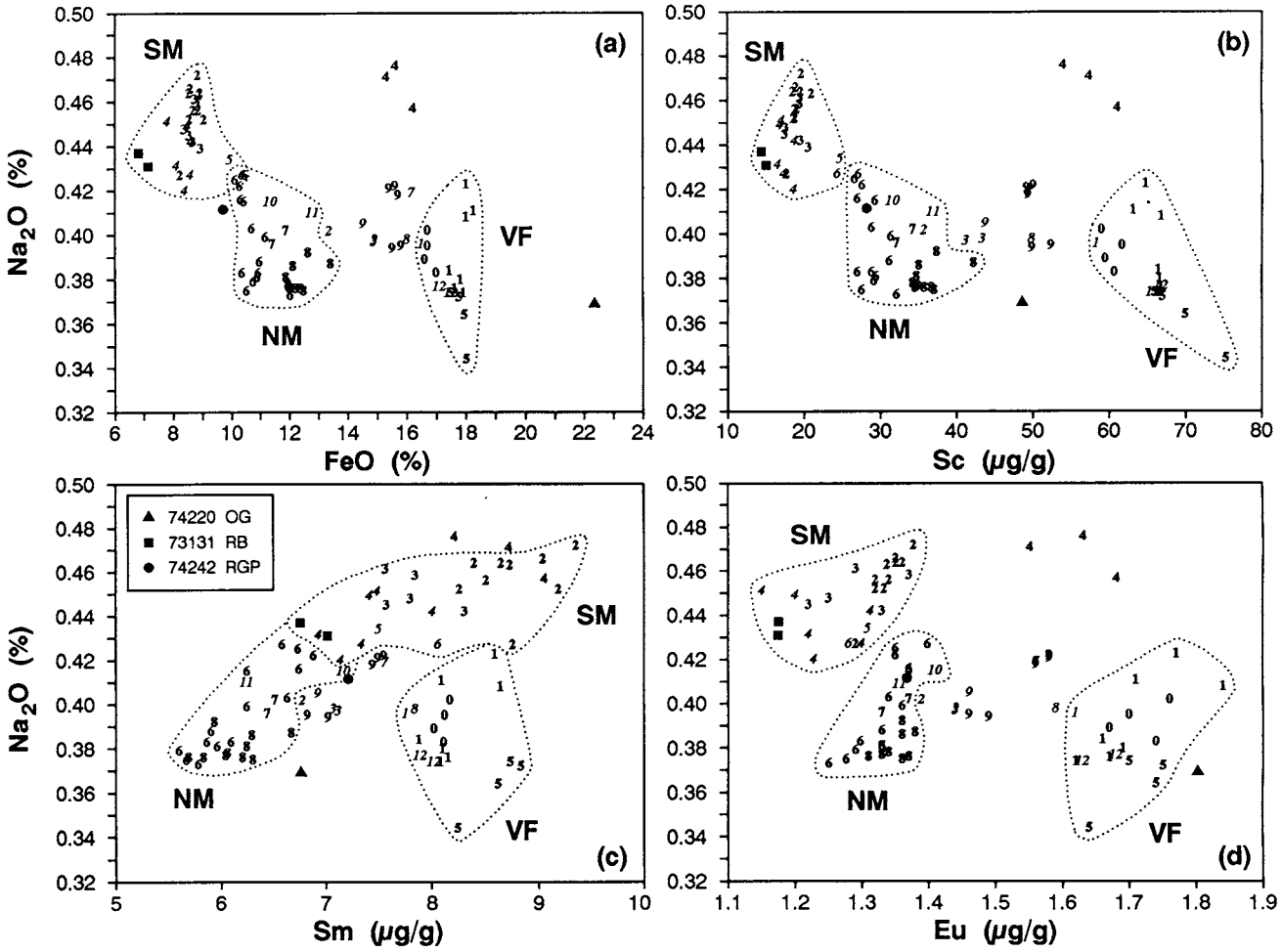

Fig. 4. Like Fig. 3, except for Na_2O.

tions at the low end of that range. Other station 3 soils have even lower ITE concentrations (Fig. 3; *Wänke et al.,* 1974). As discussed below, one of the two splits of 73211 is anomalously enriched in rare earth elements (REE). The two well-studied soils from station 2A (73121 and 73141) also have lower ITE concentrations than those of soils from nearby station 2 (*Laul et al.,* 1974; *Wänke et al.,* 1974). Two splits each of two previously unstudied samples from station 2A were analyzed here. One of the samples (73131) is not a true soil, but a friable regolith breccia that is discussed in more detail below. For the other (73151) the two splits differ by 10-15% in ITE concentrations.

Soils consisting largely of ejecta from fresh craters often contain coarse-grained, poorly mixed material and consequently often differ in composition from nearby mature regolith. At station 1, the two samples collected on the wall of a 10-m blocky crater (71041 and 71061) are among the most immature and coarse grained of Apollo 17 soils (*McKay et al.,* 1974; *Morris et al.,* 1983). Compared to the other three station 1 soils, the immature soils have higher concentrations of the Na_2O and Eu (1.09-1.07 times enriched) and REE (1.02-1.05 times), although concentrations of major and compatible trace elements (e.g., Sc) are not anomalous. Station 5 was also located on the blocky rim of a crater on the valley floor (Camelot Crater, 0.65 km diameter). Although the two splits of soil 75061 differ considerably in composition, both are richer in Sc than the other station 5 soil, 75081. These two soils have the highest concentrations of Sc of all Apollo 17 soils (Fig. 3), indicating that the station 5 soil contains the largest component of mare basalt and consequently the least highland material (Fig. 5). Both soils are submature and probably contain a large component of ejecta from Camelot Crater (*Morris et al.,* 1983; *Wolfe et al.,* 1981).

In summary, soil samples collected from different locations or depths at a given sampling station are usually similar to each other in composition, but differences that are significant compared to analytical precision do occur. Most of the differences in lithophile-element concentrations among 50-mg splits of <1-mm fines from a given station are less than 10% and are probably due to sampling variations associated with large par-

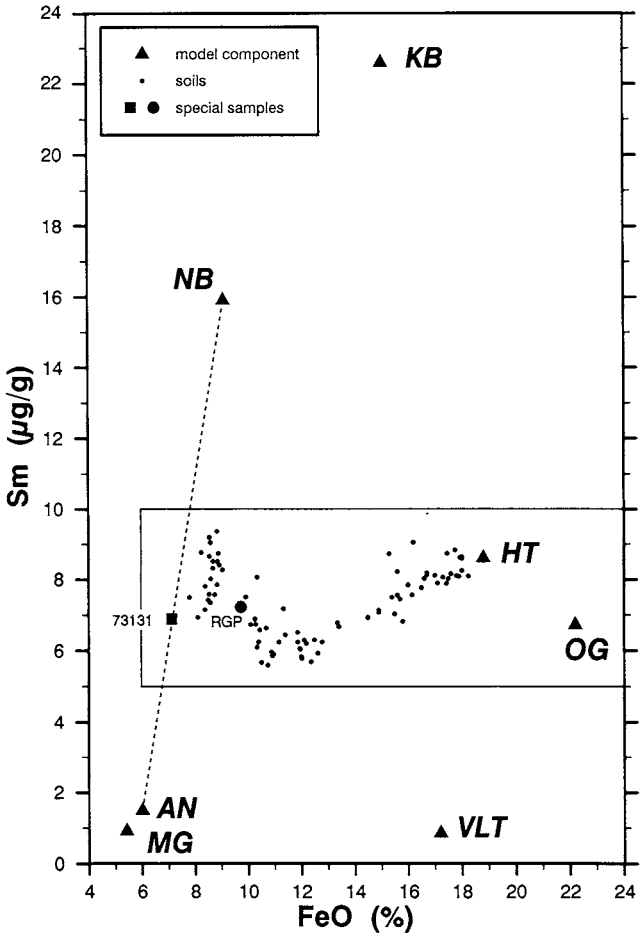

Fig. 5. Comparison of compositions of <1-mm fines (soils) and model components (Table 4). The interior box shows the range of Fig. 3a. The dashed line shows that regolith breccia 73131 is intermediate in composition between the noritic breccia (NB) and anorthositic norite (AN) components. The high-FeO components are high-Ti mare basalt (HT), orange glass (OG), and very-low-Ti mare basalt (VLT). The composition of the high-*Mg'* (MG) and KREEP basalt (KB) components are also shown.

ticles of some distinct lithology or, in some cases, small particles of extreme composition (section 3.1.3). Thus, the 50-mg splits analyzed here are not always representative of the ~100 g of <1-mm material typically obtained in a soil scoop. Differences resulting from true variation in the composition of the regolith over small lateral or vertical distances occur, but they are also not large and are often caused by fresh crater ejecta or material eroded from boulders. Such differences can usually be attributed to differences in the abundance of some compositionally distinct lithologic component.

3.1.3. Sampling error: Whitlockite, zircon, and meteoritic material. Two of the splits analyzed by INAA are compositionally anomalous because they contain high concentrations of certain ITEs. Split 73211A from station 3 is generally similar to other splits from stations 2 and 3, except that it has concentrations of light REE about a factor of 3 greater and heavy REE and Th about a factor of 2 greater (Fig. 6). Concentrations of Eu and U are also somewhat enriched, but those of Zr, Ba, Hf, and Ta are not (Table A1). Thus, the enrichment does not result from a large particle of ITE-rich melt rock, which occasionally causes ITE anomalies in Apollo 16 soils (*Korotev,* 1991), but is probably caused by the presence of a large grain of a phosphate mineral. A mixture of 99.7% typical soil from stations 2 or 3 and ~0.3% whitlockite with the composition of those reported from Apollo 14 and 16 (*Lindstrom et al.,* 1985) accounts well for the high concentrations of trivalent REE in sample 73211A; apatite such as that reported by *Lindstrom et al.* (1985) does not account well for the REE enrichment. As the split weighed 50 mg, this whitlockite would have a mass of ~0.15 mg (approximately 0.4 mm in diameter if a single grain).

The data for 73211A allow estimation of the concentrations in lunar whitlockite of Th and U, elements not determined by *Lindstrom et al.* (1985). Assuming that the sample contains exactly 0.300% whitlockite [i.e., that the trivalent REE concentrations are similar to those reported by *Lindstrom et al.* (1985)] and that the whitlockite is the carrier of the "excess" REE, Th, and U (compared to typical South Massif soil), the concentrations of these elements in the whitlockite can be calculated from mass balance (Table 3). This exercise indicates that the Th/U ratio of the whitlockite is 8 ± 1, a value greater than the ratio of 3.6 typical of high-K KREEP (*Warren,* 1989), but more similar to the ratio of 6.85 obtained for a whitlockite-rich quartz monzodiorite reported from Apollo 14 (*Jolliff,* 1991).

The single split of 79221 analyzed here contains concentrations of Zr and Hf 10.8 and 7.6 times greater, respectively, than those typical of station 9 soils (Table A1). Concentrations of heavy REE and U, but not Th, are also anomalously high in this split. These enrichments can be attributed to a 0.2-mg grain of zircon (0.4-0.5 mm diameter) with a Zr/Hf ratio of

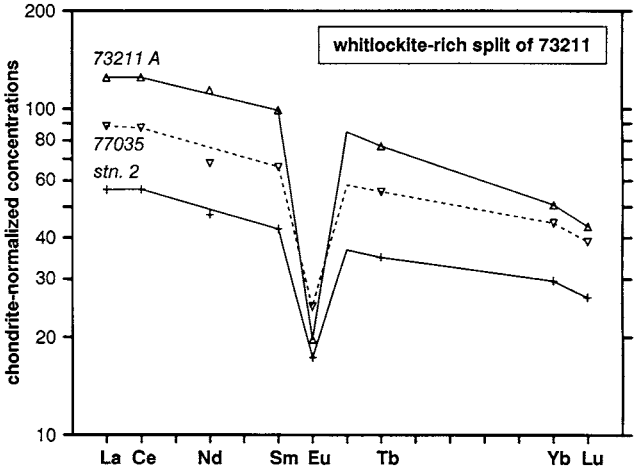

Fig. 6. Concentrations of REE, normalized to volatile-free CI chondrites (Table 4), for typical station 2 soil, whitlockite-rich soil sample 73211A, and a typical noritic impact-melt breccia, 77035 (R. L. Korotev, unpublished data, 1991).

TABLE 3. Estimated concentrations (in μg/g) of some incompatible trace elements in the whitlockite in anomalous sample 73211A, assuming a 0.300% component of whitlockite, and comparison to other lunar whitlockites.

	73211A	14321* n=4	14305* n=1	67975* n=2
La	7,410	7,702	8,700	10,760
Ce	19,400	20,624	21,912	28,430
Nd	14,000	12,476	11,662	17,108
Sm	3,850	3,315	2,827	4,608
Eu	61.5	17.3	41.0	71.0
Tb	685	569	471	788
Yb	1,550	1,903	1,252	3,020
Lu	193	224	208	351
Th	510	n.a.	n.a.	n.a.
U	60	n.a.	n.a.	n.a.

* Mean data from *Lindstrom et al.* (1985), where n is the number of analyses. The value of 0.300% was chosen arbitrarily, but so the absolute concentrations were similar to those for the whitlockite from the Apollo 14 samples of *Lindstrom et al.* (1985). n.a. = not analyzed.

49 in the 50-mg split. This Zr/Hf ratio is typical of zircons from Apollo 14, where most lunar zircons have been obtained (*Meyer et al.*, 1991). Another station 9 sample, a soil from drive tube 79001/2, also contained anomalously high concentrations of Zr and Hf (*Morris et al.*, 1989).

Although data for siderophile elements Ni, Ir, and Au are imprecise, split 76031A is significantly enriched in these elements, as well as Fe and Co (precisely determined), compared to split 76031B and all other soils. Because the Ni concentration of 76031A is 990 μg/g, whereas the concentration does not exceed 400 μg/g in any other sample, the excesses are probably carried by a single particle (section 4.13).

3.2. Regolith Breccia 73131

Sample 73130 was collected as a friable regolith breccia from a 3-m-diameter blocky crater at station 2A (LRV-4). Before processing in the lunar receiving lab, the breccia disintegrated and was subsequently treated as a soil; i.e., it was sieved and the grain-size fractions given "soil" sample numbers (73131-73134). We have analyzed two splits from the <1-mm grain-size fraction, 73131, with similar results (Table A1, Figs. 3 and 4). Sample 73131 has the lowest concentrations of Sc, Cr, and Fe of all Apollo 17 soils, indicating that it has the smallest component of mare material. It also has the lowest concentrations of ITEs and siderophile elements among the South Massif soils. Sample 73131 represents one compositional extreme among the samples studied here, but it is most similar to the other station 2A soils.

4. MASS-BALANCE MODEL

4.1. Overview

In the discussion above, differences in composition among soils were described qualitatively in terms of differences in the proportions of lithologies found in the regolith. Such differences were first explained quantitatively by *Rhodes et al.* (1974) in terms of a mass-balance ("mixing") model in which Apollo 17 soil compositions were described by mixing four lithologic components in the proportions that best accounted for the observed composition of the soil. In this section, we apply a similar strategy, but modified for a larger number of chemical elements and more recent information on Apollo 17 lithologies and their compositions. Principal model assumptions involve the nature, number, and composition of the components, while model predictions are the best-fit mass fraction of each of the components and the composition of the best-fit mixture.

Apollo 17 soils, of course, contain more than four compositionally distinct components. *Heiken and McKay* (1974) classified 21 petrographically distinct components in these soils, many of which span a range of compositions ("norite," "plagioclase") and others that can be represented by several different compositions (e.g., "basalt" and "other"). From the mathematical standpoint, the mass-balance calculations used here could include up to 27 components because 27 chemical elements are modeled. In practice, results of such a model would provide little useful information. The goodness of fit (section 4.8) is not significantly improved by addition of more than six to eight components because most of the components are volumetrically minor and compositionally indistinct and some components (basalt) are composed of others (plagioclase, pyroxene). Therefore, any number of solutions can provide equivalently good fits to the data. Also, the 27 chemical elements do not represent 27 independent parameters because concentrations of any given element correlate with those of a number of other elements (e.g., the ITEs) to some degree among the components. Thus, it is impractical to start our modeling exercise by including components representing all lithologies observed in the soils. Instead, we start with a small number of components and add other likely components until reasonable mass balance is achieved and no significant improvement in fit is obtained.

Because it has been judged successful in the past, we start by testing the four-component model of *Rhodes et al.* (1974). We show that model to be quantitatively inadequate. Based on the results of that model, we make a series of assumptions about additional components that improve the quality of the fit and arrive iteratively at a new model that better accounts for the compositions of the soils. The new model provides some geologic insight not provided by previous models. We stress that although the final model provides a solution that is a good fit to the composition of most soils, it is not a unique solution because of the variety of possible input assumptions. To emphasize that point, in the following section we show how differences in input data and assumptions of previous models have led to substantially different model predictions for Apollo 17 soils. We believe that our model is more realistic because it is based on a larger dataset, the assumptions are defendable, and results are more consistent with petrographic data, although petrographic data cannot be used to rigorously test the model (section 4.2).

4.2. The Four-Component Model

We designate the four components of *Rhodes et al.* (1974) HT for high-Ti mare basalt, OG for 74220-type orange glass, NB for noritic impact-melt breccia, and AG for anorthositic

gabbro. The four-component model of *Rhodes et al.* (1974) has been regarded as successful at accounting for the compositions of Apollo 17 regolith samples and has been applied by others in its most general form to different datasets (*Korotev,* 1976; *Laul et al.,* 1979; *Laul and Papike,* 1980; *Laul et al.,* 1981; *Morris et al.,* 1989). Although the fundamental assumptions and arithmetic calculations of each of these modeling exercises have been similar, results have often been substantially different and in some cases geologically unreasonable. For example, estimates for the abundance of the MB component in station 2 soils (South Massif) are considerably different from each other: -4.1%, 1.8%, and 5% based, respectively, on the models of *Laul et al.* (1981), *Rhodes et al.* (1974), and *Korotev* (1976). As another example, estimates for the abundance of OG component in <1-mm fines from station 6 have been high [11.7% by *Rhodes et al.* (1974) and 17.6% by *Laul et al.* (1981)] compared to the abundance of orange and black pyroclastic glass observed petrographically [5 ± 3%, mean and standard deviation of nonagglutinate portions of 90-150-μm grain-size fractions of five samples (*Heiken and McKay,* 1974)]. *Caveat:* The abundance of a "chemical" component estimated from mass-balance models for <1-mm fines cannot in general be expected to compare well with the abundance of the corresponding "petrographic" component from modal analysis. For practical reasons, modal analysis is done on coarser grain-size fractions and the distribution of some components varies with grain size. For example, modal analysis of the soils by *Heiken and McKay* (1974) was usually done on 90-150-μm grain-size fractions, but the orange glass has a mean grain size below this range (~40 μm; *McKay et al.,* 1974). Also, not all of a "chemical" component is identifiable petrographically because it is camouflaged in agglutinates and regolith breccias (which make up 30-60% of the 90-150-μm fraction of most soils) and individual mineral grains (10-30%); the "petrographic" component from which the mineral grains derive is not usually identified (data from *Heiken and McKay,* 1974).

The differences in results obtained by different modelers arise from several causes. First, different sets of elements were modeled in each case and the concentrations of these elements were determined with varying degrees of analytical precision. Modeling by *Rhodes et al.* (1974) depended primarily upon mass balance for major elements and was further constrained by a few trace elements determined by XRF analysis (Sr, Y, Zr). However, a characteristic of the Apollo 17 mixing components is that they vary considerably in both relative and absolute concentrations of the REE (Fig. 7). The two highland components, NB and AG (AN in Fig. 7; see section 4.4), have significantly different REE abundances. The relative depletion of light REE in the HT and OG components contrasts strongly with the relative enrichment observed in the highland components. The OG component is relatively depleted in heavy REE compared to the HT component. Thus, the REE provide a strong and independent constraint on mass balance. This is why the models of *Korotev* (1976) and *Morris et al.* (1989), which were constrained only by INAA data for REE and a few other elements (primarily Na, Sc, Fe, and Cr), are still relatively successful because the REE "pattern" for a soil is a linear combination of those for each of the four model components.

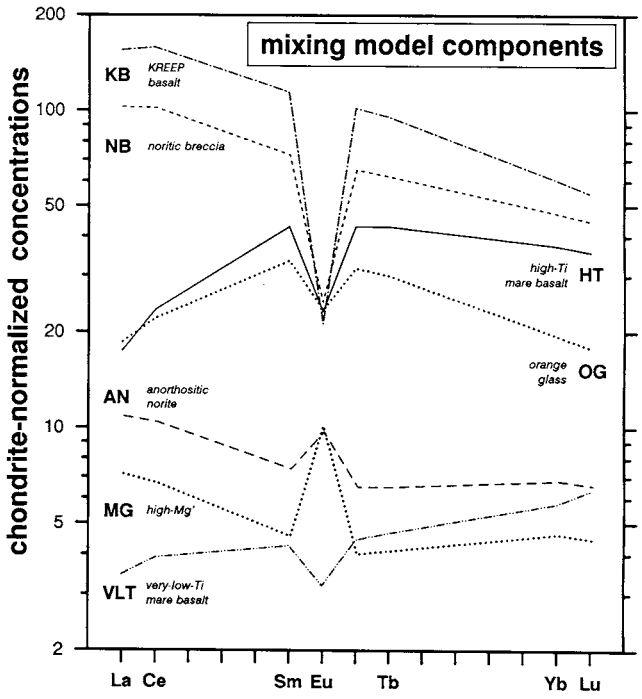

Fig. 7. REE concentrations (normalized to concentrations in volatile-free CI chondrites) in mixing model components as a function of atomic number (data and sources listed in Table 4).

Mass-balance models are best constrained with a relatively full suite of elements, such as that used by *Laul et al.* (1979), *Laul and Papike* (1980), and *Laul et al.* (1981). However, major elements must be determined precisely, and in those studies data for Mg and Ca (obtained by INAA) were not precise. Magnesium is a critical element in mass-balance models because the Mg/Fe ratio is a strong constraint on the ratio of mare to highland components (Table 4). To help alleviate these problems in the model presented here, the model is constrained by a large number (27) of major, minor, and trace elements (including REE), most of which are determined with reasonably high precision.

A second reason that different modelers obtain different results is that sampling precision may be worse than analytical precision for some elements because of the small masses typical of lunar sample analysis. For a 50-mg sample of <1-mm fines (a typical mass), a single particle 1 mm in diameter (not uncommon) accounts for 3% of the mass of the sample. It is unlikely that any individual soil particle will have the exact composition of one of the model components. Thus, we have modeled average compositions of several samples whenever possible.

Third, although the four components of previous modeling exercises have been nominally the same, the compositions used to *represent* those components have differed. This is probably the single greatest cause of variation among results of previous models. The concept of an "OG component" is reasonable because different samples of orange glass are nearly indistinguishable in composition, but samples of "anorthositic

TABLE 4. Compositions of mixing-model components and uncertainties used for weighting factors (σ_i).

		Mare			KREEP	Highland			Vol.-free	σ_i
	Unit	HT	VLT	OG	KB	NB	AN	MG	CI	
SiO_2	%	38.8	48.6	38.6	49.7	46.6	44.7	45.6	31.0	0.25
TiO_2	%	12.3	0.7	8.76	1.25	1.56	0.55	0.10	0.1	0.2
Al_2O_3	%	8.93	10.8	6.53	13.6	18.2	25.5	20.14	2.23	0.15
FeO	%	18.8	17.2	22.2	15.0	9.09	6.00	5.41	33.3	0.15
MgO	%	8.42	11.7	14.39	9.5	12.17	7.79	16.8	22.3	0.10
CaO	%	10.86	9.7	7.69	10.2	11.25	14.94	11.16	1.77	0.10
Na_2O	%	0.393	0.17	0.366	0.441	0.643	0.314	0.264	0.917	0.005
(*Mg'*)	%	44.4	54.8	53.6	53.0	70.5	69.8	84.7	54.4	—
Sc	μg/g	82	53	48.3	47.6	17.0	13.7	5.6	7.9	0.5
Cr	μg/g	3200	5730	4650	3390	1340	1224	1335	3620	30
Co	μg/g	20.0	37.0	61.5	36.0	30.8	26.9	41.2	693	4
Ni	μg/g	2	2	113	60	280	107	24	14960	50
Sr	μg/g	174	40	205	95	207	112	112	11	25
Zr	μg/g	200	20	184	563	480	40	30	5	25
Ba	μg/g	67	50	78	402	360	74	46	0.3	15
La	μg/g	5.57	1.1	5.94	49.1	34.2	3.45	2.27	0.32	0.1
Ce	μg/g	19.3	3.2	18.1	128.	88.	8.52	5.48	0.82	0.7
Sm	μg/g	8.6	0.85	6.71	22.6	15.9	1.48	0.91	0.20	0.1
Eu	μg/g	1.77	0.24	1.79	1.60	1.96	0.735	0.77	0.076	0.04
Tb	μg/g	2.12	0.23	1.48	4.64	3.18	0.32	0.202	0.049	0.05
Yb	μg/g	8.25	1.27	4.31	13.2	11.3	1.50	1.02	0.22	0.1
Lu	μg/g	1.18	0.21	0.59	1.80	1.52	0.217	0.147	0.033	0.015
Hf	μg/g	7.8	0.69	5.77	16.7	11.4	1.78	0.59	0.14	0.15
Ta	μg/g	1.8	0.05	1.00	1.50	1.50	0.19	0.10	0.02	0.07
Ir	ng/g	0.01	0.01	0.7	0.1	9.0	2.4	0.3	654	1
Au	ng/g	0.01	0.01	0.3	0.1	4.2	1.2	0.1	190	1
Th	μg/g	0.4	0.06	0.42	5.5	5.1	1.04	0.29	0.04	0.06
U	μg/g	0.15	0.02	0.13	1.45	1.4	0.36	0.09	0.011	0.1

The composition of the high-Ti mare basalt (HT) component was derived from the large datasets of *Rhodes et al.* (1976) and *Warner et al.* (1979); concentrations for some trace elements were estimated. The VLT component is based on three small samples described by *Wentworth et al.* (1979); concentrations for some trace elements were estimated. Data obtained here for 74220 (Tables A1 and A2) were averaged with those of *Rhodes et al.* (1974) and *Duncan et al.* (1974) for the orange glass (OG) component. The KREEP basalt (KB) component derives from nine subsamples from 72275 (*Salpas et al.*, 1987). The NB component is based on the noritic breccia component of *Rhodes et al.* (1974), samples 77035 and 72395 (*Wänke et al.*, 1975, and R. L. Korotev, unpublished data), and sample 72244 (*Warren et al.*, 1991). The noritic anorthosite (NA) component is a composition calculated from sample 73131 (Table 2) assuming that 73131 is a mixture of 37% NB and 63% AN components; see text. The high-*Mg'* (MG) component is a mixture of 60% troctolite and 40% norite and is based primarily on data for 76535 and 78255 of *Haskin et al.* (1974), M. M. Lindstrom (unpublished data), and *Warren and Wasson* (1979) [also *Winzer et al.* (1975) for 78235]. Concentrations for the volatile-free, CI-chondrite component are the values of *Anders and Grevesse* (1989) for C1 chondrites multiplied by 1.36. The values σ_i approximate 1σ analytical uncertainties; weighting factors for the mixing model are σ_i^{-2} (*Boynton et al.*, 1975).

gabbro," for example, are highly variable in composition (section 4.4). In this study we derive component compositions by averaging many data from a variety of sources, although we must resort to some assumptions and compromises for some components.

Fourth, the numerical modeling techniques, although nominally similar (least-squares), have differed in detail, most notably in how (or if) weighting factors for the various elements were used and what (if any) criteria were used to judge model success (goodness of fit). In our model, elements determined with high precision have more influence than elements determined with poorer precision. We judge the model success by comparing observed and predicted concentrations and seeking patterns in the differences. We also consider whether the results are geologically realistic, i.e., the model should predict that components have positive abundances within model uncertainty, that best-fit abundances of components be similar for soils of similar composition, and that the sum of the components total 100%.

4.3. Component Compositions and Model Calculations

We have calculated new average compositions with emphasis on samples for which major- and trace-element data were obtained on the same sample. A volatile-free, CI-chondrite component (CI) was included to account for siderophile elements (*Boynton et al.*, 1975), although Ni, Ir, and Au are each determined imprecisely. Component compositions and their sources are listed in Table 4; derivation of the composition of the anorthositic norite component is discussed elsewhere (section 4.4).

We used the weighted least-squares modeling calculations described by *Boynton et al.* (1975) to find the proportions of the components that best accounted for the station-average compositions of Table 2. All the elements determined here were included in the modeling except Nd, which is imprecisely determined compared to the other REE. Weighting factors, σ_i^{-2} of *Boynton et al.* (1975), were based primarily on analytical uncertainties associated with the analysis of a

single sample. For the six major elements determined here, we used one-half of the 95% uncertainties (i.e., effectively 1σ) listed in Table A2 for the value σ_i. For the elements determined by INAA, we used the 1σ uncertainties listed in Table A1. The exceptions to this rule were Zr and Sr for which 0.5σ, not 1σ, uncertainties were used. When available, the station averages of Table 2 for Zr and Sr favor XRF data because these two elements are determined imprecisely by INAA. Thus, Zr and Sr averages in Table 2 are usually more precise than implied by the uncertainties of Table A1. A factor that cannot be rigorously treated by the model is that some of the "averages" of Table 2 include results of several analyses and/or several samples whereas others, particularly those for LRV stops, are not averages but simply the results of a single analysis.

4.4. "Anorthositic Gabbro" and Anorthositic Norite

Although the mare components of the model each represent igneous, monomict lithologies, both of the highland components represent polymict rocks. Samples of the predominant poikilitic impact-melt breccia from Apollo 17 are relatively uniform in composition (*Spudis and Ryder,* 1981), but samples with the general composition of the "anorthositic gabbro" component of *Rhodes et al.* (1974) are more variable in composition. Most samples of "anorthositic gabbro" are granulitic or impact-melt breccias that have been separated as clasts from large noritic impact-melt breccias or that occur as small particles in the soil. Values of *Mg'* [mole percent Mg/(Mg + Fe)] in granulitic breccias from Apollo 17 span a large range and the concentration ratio $(FeO + MgO)/Al_2O_3$ is also variable (*Lindstrom and Lindstrom,* 1986; *Salpas et al.,* 1988). The absolute and relative concentrations of Fe and Mg in the AG component have a strong effect on the absolute and relative proportions of HT and OG components required by the model for best fit.

In preliminary modeling, we experimented with various "anorthositic gabbro" components based on literature data (*Lindstrom and Lindstrom,* 1986; *Salpas et al.,* 1988; *Warren et al.,* 1991). However, no AG component we tried provided good fits to the Ti-poor, feldspathic soils from the South Massif (e.g., for stations 2, 2A, and 3, χ^2/ν values ranged from 5 to 8; section 4.8). Instead of "fishing" for an AG composition we calculated a composition using the following procedure. We inferred from the composition of 73131 that it had a large AG component (Fig. 5). Because 73131 is a regolith breccia from the South Massif composed of fine-grained material, we assumed that its AG component was representative of the AG component of the South Massif soils. We also assumed that 73131 was composed only of NB component and "anorthositic gabbro" component, with no contamination by mare material. A two-component model using only the NB component and any of several experimental AG components provided good fits to the ITEs in 73131 with about 37% NB component. We then calculated the composition that, when mixed with the NB component in a 63:37 ratio, provided ideal agreement to the composition of regolith breccia 73131. [We also included a small fraction of CI component to account for siderophile elements and adjusted concentrations of the trivalent REE slightly to produce smooth variation with atomic number of the CI-normalized values (Fig. 7).]

The calculated composition, which we designate AN for anorthositic norite (Table 4), is within the range of Apollo 17 granulitic breccias (*Lindstrom and Lindstrom,* 1986; *Salpas et al.,* 1988), but is somewhat more mafic than "anorthositic gabbro" components used in previous models [$Al_2O_3 = 25.5\%$, compared to 26.5% (*Rhodes et al.,* 1974) and 26.6% (*Laul et al.,* 1979)] and the TiO_2 concentration is slightly greater [0.55%, compared to 0.31% (*Rhodes et al.,* 1974) and 0.41% (*Laul et al.,* 1979)]. This suggests that our assumption that 73131 contains a negligible amount of mare component may be incorrect. However, based on a comparison of TiO_2 and REE data (shape of "REE pattern"; Fig. 7) for the AN component and rocks of similar composition with no mare component, 73131 cannot contain more than about 1.5% HT component, so the assumption is justifiable. Because *Mg'* for 73131 (70.1) and the NB (70.5) component are both about 70, the *Mg'* of the AN component is also about 70 (69.8, Table 4). This is an intermediate value for Apollo 17 granulitic breccias (*Lindstrom and Lindstrom,* 1986) and slightly greater than that of the AG component of *Rhodes et al.* (1974) (*Mg'* = 68.6). We note that the AN component is similar in composition to lunar meteorite Y-791197, although the *Mg'* is less in the meteorite (65.5) (*Warren and Kallemeyn,* 1986; *Ostertag et al.,* 1986; *Lindstrom et al.,* 1986).

When normative mineral concentrations are calculated from the composition of the AN component and the mass percentages converted to volume percentages, a component with 76% plagioclase, 11% orthopyroxene, 4% clinopyroxene, and 8% olivine is obtained. A lunar rock with these modal percentages is classified as an anorthositic norite, thus the designation AN. However, the estimated modal composition is very near the "corner" of its field in the appropriate classification diagram (*Stöffler et al.,* 1980). Applying this same procedure to the "anorthositic gabbro" component of *Rhodes et al.* (1974) yields a noritic anorthosite.

We have substituted the AN component for the AG component of *Rhodes et al.* (1974) in the model presented here. Using the AN component significantly improves model results for all South Massif soils and values of χ^2/ν (section 4.8) are equivalent to those obtained at other stations.

4.5. VLT Basalt and the MB Component

Compositions of best-fit mixtures derived from the model based on the HT, OG, NB, AN, and CI components consistently had larger TiO_2 concentrations than actually observed in the soils and the absolute magnitude of the excess increased with the fraction of HT component. For example, for the LM/ALSEP station average, the observed TiO_2 concentration is 8.47% (Table 2), whereas the best-fit combination of components resulted in 9.08%, a factor of 1.07 greater. This result is not a peculiarity of our model, but also occurs in the models of *Rhodes et al.* (1974) (factor = 1.04 for LM/ALSEP soils) and *Laul et al.* (1979) (factor = 1.16 for >90-μm fractions of four 70005 soils). The overestimation of TiO_2 by the model suggested that the actual mare components of the soils are not

as Ti-rich on average as the best-fit mixtures of HT (12.3% TiO_2) and OG (8.8% TiO_2) components. As the average TiO_2 concentrations of typical high-Ti mare basalt and orange glass are well established, the model results could only be improved by inclusion of an additional mare component with a low TiO_2 concentration. We considered two likely components. First, fragments of VLT basalt (very low Ti, <1% TiO_2) occur in the deep-drill core at the LM site (*Vaniman and Papike,* 1977a; *Taylor et al.,* 1977; *Wentworth et al.,* 1979). Second, a recently described "variant" of high-Ti basalt, based on a sample from regolith core 79001 (station 9), contains a lower concentration of TiO_2 (9.9%) than typical high-Ti basalt (12-13%) (*Ryder,* 1990). As a test, components representing both types of basalt were included individually in the model along with the HT and OG components. No significant improvement was obtained with the 79001 basalt; TiO_2 concentrations were still overestimated. However, inclusion of the VLT basalt component (Table 4) significantly improved the results. Therefore, we assume that VLT basalt is a significant component of the Apollo 17 regolith and have included it as a component in the mass-balance model. However, we do not tabulate here the results of the model in which the VLT basalt was used as a discrete component. Instead, we present results using a single mare basalt component that is a mixture of 92% HT component and 8% VLT component. Reasons for that choice are discussed next.

For soils containing >50% total mare-basalt component (HT + VLT), the ratio VLT/(HT + VLT) in the model results averaged 0.08. This means that the average composition of the basalt-rich soils is matched best by a component of mare basalt that is 8% VLT and 92% HT. Eight percent may seem rather high considering the virtual absence of VLT basalt among the returned rocks and rake samples. However, all samples of VLT basalt from Apollo 17 are small, which indicates that the particle-size distribution of the VLT basalts is finer than that of the high-Ti basalts (perhaps the VLT basalts are older; no age data are available). Therefore, it is not unreasonable that the occurrence of VLT basalt in the <1-mm fines is as high as 8% of the total mare basalt component. For soils with >50% total mare-basalt component, model results for the percentage of VLT component ranged from 2.2% (LRV-12) to 6.6% (station 9) with a mean of 4.6% and absolute standard deviation of 1.7%. The latter value (1.7%) is the same as the 1σ model uncertainty in the abundance of VLT component (1.6%, based on goodness of fit). Therefore, differences predicted by the model for the abundance of VLT component among valley-floor stations are not significant and the model results do not provide any information about variation in the relative distribution of VLT basalt with site geography.

The relatively large degree of scatter in the fraction of VLT component predicted for basalt-rich soils indicated that model results for the basalt-poor soils were even less reliable. For example, the model predicted 4.4 ± 0.9% VLT component in the station 2 soils and 0.3 ± 1.9% for the station 3 soils, even though soil compositions at both stations are similar. Therefore, we have modified the model by making the assumption that the ratio VLT/(HT + VLT) is 0.08 for *all* stations and derive a new component that is a mixture of 92% HT and 8% VLT components. This component, designated MB for mare basalt, was used in the final model instead of the discrete HT and VLT components.

4.6. High-*Mg'* Components in North Massif and Sculptured Hills Soils

The mass-balance model, as modified above (MB + OG + NB + AN + CI), accounted well for the compositions of most soils. However, a mismatch outside the range of analytical uncertainty occurred for soil from station 6 (North Massif). Station 6 soil has a higher concentration of MgO (1.08×) and lower concentrations of FeO (0.96×) and Cr (0.92×) than the best-fit model composition. To a lesser extent these same problems occurred for soils from stations 7 and 8. The underestimation of MgO concentrations for North Massif soils was also noted by *Rhodes et al.* (1974), who suspected the presence of "an additional high-magnesian component such as dunite or troctolite," although they did not specifically include such a component in their model.

This result is not surprising, as most of the samples of plutonic norite, troctolite, and their more anorthositic variants returned from the Apollo 17 site were found at stations 6, 7, and 8. As a test, components representing troctolite (sample 76535), anorthositic troctolite (76335), or norite (samples 77075 and 78255, which differ considerably in *Mg'*) were each included individually in the model for the station 6 soil [component compositions primarily from data of *Warren and Wasson* (1978, 1979)]. Each of these components improved the fit, and the required proportions ranged from 11% for troctolite 76535 and norite 77075 to 32% for troctolitic anorthosite 76335. We take this as strong evidence that soils from the North Massif contain a significant component of material derived from the "Mg suite" of lunar plutonic rocks. Although troctolite 76535 provided a better fit than any of the other components tested, particularly for Fe, Mg, and Cr, it seemed unreasonable to model the high-*Mg'* component as a single lithology when other such components are known to occur. Including troctolite and one of the other high-*Mg'* components improved the fits even further, but often the best-fit solution included negative concentrations of one or more components because the model is not sufficiently constrained to realistically distinguish among such a large number of mafic components (MB, OG, NB, and two high-*Mg'*) when the total fraction of mafic components is only about 50%. At station 6, which required the highest concentration of high-*Mg'* components in all of the models, 9% troctolite 76535 and 6% norite 78255 provided a slightly better fit than troctolite alone. Thus, a single high-*Mg'* component was included that represented a mixture of 60% troctolite 76535 and 40% norite 78255, the proportions that worked best at station 6. This component is designated MG.

For all stations other than those from the North Massif and Sculptured Hills, the predicted proportion of MG component averaged -0.4 ± 2.0% and there was no indication that the MG component was present in proportions significantly exceeding the model uncertainty at any other region of the site, even at the South Massif. For example, the model predicted -3.0 ± 2.4% and 3.8 ± 3.0% MG component, respectively, for the station 2 and station 3 soils. Thus, we have included the MG

component in the model only for the five stations from the North Massif area. We judged it unrealistic to include the component for all soils, although it mathematically improved some fits, because the improvements were negligible and the implications were geologically misleading.

4.7. Apollo 17 KREEP Basalt

Although the station 2 composition (Table 2) is based on 10 analyses of 5 different samples, the model (MB + OG + NB + AN + CI) provided a poorer fit for station 2 (χ^2/ν = 3.0, Table 5) than for most other stations where the modeled composition is the average of many samples (section 4.8). Suspecting another "missing component," we remodeled the South Massif soils including a component of KREEP basalt because clasts of KREEP ("pigeonite") basalt have been found in sample 72275 from boulder 1 at station 2 (*Blanchard et al.,* 1975; *Salpas et al.,* 1987). This lithology is compositionally distinct and is characterized by high concentrations of ITEs and a major-element composition intermediate to those of the mare and highland components (Fig. 5). Inclusion of the KB component (KREEP basalt; Table 4) improved the goodness of fit, but only for the station 2 soils; best fit was obtained with 4.3 ± 1.2% KB component (Table 5). (For comparison, at stations 2A and 3 the model predicted 1.5 ± 0.8% and -1.6 ± 1.6% KB component with no improvement in χ^2/ν.) Predictably, the abundance of NB component decreases from 47% to 42% by addition of the KB component because both components have high ITE concentrations. These results suggest that KREEP basalt such as found in breccia 72275 is a volumetrically minor but compositionally important component of the station 2 soils.

Among station 2 soils, the highest concentrations of ITEs occur for the three soils collected as fillets from boulder 1, from which 72275 was collected (section 3.1.2). The model, when applied to the fillet soils and other station 2 soils separately, suggests that the ITE enrichment in the fillet soils is caused by KREEP basalt, not ITE-rich noritic breccia. This cannot be tested rigorously, however, because major-element data are available only for one sample of fillet soil (Table A2, 72241).

4.8. Goodness of Fit

Results of the final model are presented in Table 5 for the station mean compositions of Table 2. Values of χ^2/ν (reduced chi-square; *Boynton et al.,* 1975) are tabulated for each station mean; these values are a measure of the goodness of fit, with lower values indicating better fits. If the soils were in fact perfect mixtures of the assumed components and analytical uncertainty were the only source of error, then the χ^2/ν values would approximate unity on the average. Because these conditions are not met in reality, χ^2/ν values are typically >1. As anticipated, better fits are achieved for soil compositions that are averages of several analyses because sampling uncertainty affects goodness of fit at least as much as does analytical uncertainty. If the weighting factors had taken sampling uncertainty into effect, the values σ_i would be at least twice as large (on average) for most lithophile elements (Table 4) [based on analyses of seventeen 50-mg samples of the very fine-grained soil at the top of the 79001/2 drive tube; *Morris et al.* (1989)]. This would have yielded χ^2/ν values about a factor of 4 smaller than those obtained here. Therefore, with certain reservations discussed below, we take χ^2/ν values of ~4 to indicate that a good fit has been achieved for compositions based on few samples (LRV stops) and expect χ^2/ν in the range of 2-3 for compositions based on several samples (e.g., stations 1 and 2).

Interlaboratory bias is another cause of high χ^2/ν values. Although most of the soil data were obtained in this laboratory, compositions of the components were taken mostly from literature sources. Except for the station 5 samples (section 4.10), the two worst fits occur for LRV-2 and LRV-6, each of which is based on a single sample (72141 and 74121) for which only one analysis (INAA) each is available, and those analyses were done in another laboratory. Other specific causes of failure by the model to reproduce precisely the soil compositions are discussed in the next five sections. In order to demonstrate in a more straightforward way than implied by the χ^2/ν values how well the model results fit the data, observed and estimated soil compositions are compared in Table 6 for four stations where data from several analyses and samples were averaged. These soils cover the range of observed compositions.

4.9. Na Enrichment in Gray Soil from Station 4

The largest discrepancy between observed and estimated compositions is for the Na concentrations in the two samples of "gray" soil from station 4 (74241 and 74261). For all other elements the model fits for those samples is good. However, for Na the observed mean concentration (0.470% as Na_2O) is 1.11 times the model-estimated concentration (0.425%). The Na enrichment is most likely caused by vapor-phase condensation because the excess Na is associated with the finest material. For the 90-150-μm grain-size fraction of 74261, the Na concentration is essentially the same as predicted by the model (0.42% Na_2O), whereas for the <20-μm fraction, it is 1.55 times enriched (0.65% Na_2O) (*Korotev,* 1976). Also, *Baedecker et al.* (1974) noted that both 74241 and 74261 were richer in Zn and Ga than any Apollo 17 soil except 74220; all three samples were collected from the same trench at station 4 on the rim of Shorty Crater. They assumed that the enrichment resulted from a large component of pyroclastic orange glass because the orange-glass spherules have high concentrations of vapor-deposited volatile elements on their surfaces as a result of their formation in volcanic "lava fountains" (*Heiken et al.,* 1974; *Meyer et al.,* 1975). However, the mixing-model results indicate that the gray soil contains a lower abundance of orange glass than most similarly mafic soils (5.3%; Fig. 8a) and the fraction of orange and black glass observed petrographically in the 90-150-μm grain-size fractions is also low (4-10% of nonagglutinate portion; *Heiken and McKay,* 1974). Volatile enrichment in the gray soil may result from remobilization of volatiles previously associated with the orange glass (section 5.2). Because the Na enrichment is probably not the result of a mixing process involving lithologic

TABLE 5. Mixing-model results: Proportions of components (in percent) resulting in best fit to station-mean compositions of Table 2 (arranged approximately in order of decreasing mare basalt abundance).

Station/Sample	χ^2/ν*	MB†	OG	KB‡	NB	AN	MG§	CI	Sum
5 (75061)	7.8	86.2	6.4		6.0	2.1		-0.1	100.6
5 (75081)	7.3	78.2	6.2		10.5	5.3		0.3	100.5
LRV-12	3.2	77.8	6.8		7.3	7.4		0.5	99.7
1	2.4	75.7	9.3		8.4	6.1		0.6	100.1
LM/ALSEP	2.9	65.5	10.5		11.0	13.2		0.6	100.7
4 (gray)	3.2	62.7	5.3		16.6	15.8		0.3	100.7
LRV-1	1.5	61.4	10.4		11.1	16.8		0.8	100.5
LRV-8	4.6	46.7	16.2		15.1	21.6		1.2	100.7
9	2.4	45.1	16.1		13.7	24.9		1.2	101.0
LRV-7	2.4	39.6	26.1		14.1	20.0		0.8	100.4
LRV-9	2.4	37.5	17.8		14.1	29.3		1.0	99.7
LRV-3	2.3	28.6	25.6		16.7	28.4		1.2	100.6
LRV-11	2.6	27.7	13.9		16.0	38.1	3.2	1.4	100.4
8	2.1	28.0	12.0		15.7	35.7	7.7	1.1	100.2
7	1.7	24.3	10.1		20.2	38.1	6.3	0.9	99.9
6	0.8	21.1	5.9		21.3	36.2	14.6	1.2	100.2
LRV-10	1.0	23.6	7.1		26.2	33.3	9.4	0.6	100.1
LRV-2	5.3	22.9	17.3		21.3	36.9		2.2	100.4
74242 RGP	3.8	19.9	1.6		28.7	49.6		-0.1	99.6
LRV-5	3.8	15.3	1.9		34.2	48.2		0.5	100.1
LRV-6	6.0	11.3	5.7		37.9	43.8		1.1	99.9
3	3.7	3.8	4.7		41.1	49.7		0.7	100.0
2	3.0	3.0	3.9		47.9	45.1		0.3	100.1
2‡	1.9	2.6	3.2	4.3	42.1	47.4		0.5	100.1
2A (LRV-4)	1.0	1.6	3.8		39.3	54.4		0.9	100.0
73131 RB	0.1	0.0	0.0		37.1	62.6		0.2	99.8
Uncertainty¶	—	1.6	1.7	1.4	0.4	1.0	1.6	0.3	2.6

* χ^2/ν = Reduced chi-square: error-weighted sum of squares of residuals divided by the number of degrees of freedom (number of elements minus number of components); these values are a measure of goodness of fit (*Boynton et al.*, 1975).

† The mare basalt (MB) component is a mixture of 92% HT and 8% VLT component (Table 4).

‡ The KREEP basalt (KB) component was included in the model only for station 2; no significant improvement was obtained by inclusion at other South Massif stations.

§ The high-*Mg*′ (MG) component is a mixture of 60% troctolite and 40% norite (see Table 4). It was included in the model for the North Massif stations only; the abundance is effectively 0 ± 2% at all other stations (see text).

¶ 1σ estimate of model uncertainty.

components, Na_2O was excluded from the model for the station 4 soils in the results presented here, hence the reasonably low reported value of χ^2/ν (3.2; Table 5).

4.10. Unidentified Components in Soils from Stations 1 and 5

Two soils were collected at station 5: Sample 75061 was collected from a depression in a basalt boulder on the edge of Camelot Crater; 75081 was collected near the base of the boulder. The model predicts that these two soils have the largest component of mare basalt of any Apollo 17 soils (75061: 86% and 75081: 78%). However, compositions of both soils are fit poorly by the model and we judge results to be quantitatively unreliable (Table 5). The high χ^2/ν values (~8) are largely due to estimated concentrations of Na_2O and Al_2O_3 that are, respectively, ~1.09 and ~0.95 times the observed values. Model predictions for the concentrations of heavy REE (Tb, Yb, and Lu) are also low by about 5%. (These are averages; the fit is worse for 75061 than for 75081.) *Mg*′ for 75061 (48.7) is greater than that of the MB (45.3) or HT (44.4) components, suggesting the station 5 soils contain an unidentified magnesian lithology or, possibly, some type of primitive basalt different from typical high-Ti mare basalt (higher *Mg*′). We have experimented by (1) substituting the individual HT and VLT components for the MB component, (2) including the MG and KB components, and (3) substituting sample 75084,11 for the AN component. [Sample 75084,11 is small troctolitic anorthosite (*Mg*′ = 75) collected with 75081 (*Warren et al.*, 1991)]. No significant improvement was obtained with any of these modifications; Na and Al concentrations were consistently over- and underestimated, respectively. Sample 75075, which is a piece of the boulder on which 75061 was collected, is a typical high-Ti basalt (*Rhodes et al.*, 1974; *Rose et al.*, 1974). Basalt 75065 and breccia 75066 collected with 75061 have not been studied.

When the mass-balance model is applied to the mean composition of the two immature soils from station 1 (71041 and 71061) the best-fit solution requires 9.4% NB component, compared to 7.9% for the mean of the other three soils from station 1, to account for the higher concentrations of Na_2O and REE in the immature soils (section 3.1.2). However, the fit is not as good for the immature soils (χ^2/ν = 4.4) as for the other three soils (χ^2/ν = 2.2). For the immature soils, the ratio of estimated to observed concentrations of La and Sm are 1.037 and 0.969, respectively (i.e., the "REE pattern" is "flatter" for the estimated composition than for the observed). This probably means that the high ITE and Na_2O concentrations in

TABLE 6. Comparison of average observed compositions with best-fit compositions estimated from mixing model for <1-mm fines from some representative stations (oxide concentration values in percent, Ir and Au in ng/g, others elements in μg/g).

Station:	1		9		6		2	
	Obs.	Est.	Obs.	Est.	Obs.	Est.	Obs.	Est.
SiO_2	39.9	40.4	42.1	41.9	43.5	43.6	45.0	45.2
TiO_2	9.63	9.61	6.39	6.91	3.35	3.47	1.50	1.54
Al_2O_3	10.85	10.57	13.89	13.94	18.25	18.25	20.7	20.6
FeO	17.75	17.55	15.35	15.14	10.73	10.51	8.72	8.64
MgO	9.64	9.54	9.98	10.08	10.76	10.75	9.93	9.97
CaO	10.8	10.7	11.2	11.3	12.1	12.1	12.8	12.7
Na_2O	0.391	0.397	0.410	0.405	0.398	0.399	0.457	0.463
Sc	66.1	67.1	50.1	49.5	28.8	29.1	19.1	19.2
Cr	3180.	3215.	2830.	2815.	1920.	1953.	1580.	1541.
Co	32.0	29.8	36.8	36.4	35.7	34.8	29.8	28.6
Ni	115.	136.	230.	267.	275.0	283.	265.	253.
Sr	166.	167.	147.	162.	155.	147.	158.	154.
Zr	215.	201.	197.	188.	183.	170.	271.	254.
Ba	115.	92.	102.	110.	129.	128.	206.	208.
La	7.43	7.58	8.68	8.79	10.13	10.24	18.3	18.4
Ce	22.8	23.2	25.2	25.1	27.6	27.4	47.9	47.5
Sm	8.24	8.10	7.26	7.26	6.21	6.18	8.74	8.84
Eu	1.71	1.62	1.53	1.48	1.33	1.25	1.34	1.34
Tb	2.07	1.92	1.76	1.65	1.41	1.34	1.71	1.80
Yb	7.47	7.26	6.24	6.07	5.02	4.95	6.45	6.35
Lu	1.04	1.03	0.871	0.853	0.700	0.690	0.889	0.866
Hf	7.26	7.08	6.04	6.18	5.01	5.01	6.83	6.71
Ta	1.32	1.49	1.03	1.16	0.76	0.81	0.84	0.86
Ir	5.5	5.1	8.4	10.0	9.7	10.5	8.4	8.4
Au	2.3	1.7	3.6	3.3	4.1	3.6	3.5	3.4
Th	0.72	0.81	1.14	1.19	1.63	1.60	3.19	2.89
U	0.22	0.26	0.34	0.36	0.44	0.48	0.79	0.82
$\chi 2/\nu$*		2.44		2.40		0.76		1.92
	%	±	%	±	%	±	%	±
MB	75.7	1.4	45.1	1.4	21.1	1.0	2.6	1.3
OG	9.2	1.5	16.1	1.5	5.9	1.1	3.2	1.4
KB	0.	0.	0.	0.	0.	0.	4.3	1.2
NB	8.4	0.4	13.7	0.4	21.3	0.2	42.1	1.6
AN	6.1	0.8	24.9	0.8	36.2	1.1	47.4	0.9
MG	0.	0.	0.	0.	14.6	1.1	0.	0.
CI	0.6	0.3	1.2	0.3	1.2	0.2	0.5	0.3
Sum	100.1	2.3	101.0	2.3	100.2	2.2	100.1	2.9

* χ^2/ν, reduced chi-square (Table 5).

the immature soils are not caused by a highland component like noritic breccia, but result instead from a component of mare basalt with higher concentrations of ITEs and Na_2O than the HT component of the model (Fig. 7). However, neither basalts 71035 or 71055 collected from a nearby boulder have unusually high ITE concentrations.

4.11. Distribution of Orange Glass

Our model results differ from those of previous models in that the estimated abundance of orange-glass component is much smaller at nearly all stations (Fig. 8a). We regard this as an improvement as the OG abundances predicted by previous models were large compared to abundances of orange and black glass observed petrographically. For example, at the LM/ALSEP station, our model predicts 10.5% OG component, which is comparable to the 7-13% orange and black glass observed petrographically (fraction of identifiable, 20-2000-μm "clasts" in top meter of the drill core; *Vaniman and Papike,* 1977b). In contrast, the model of *Rhodes et al.* (1974) predicts 16.5% and that of *Laul and Papike* (1980) predicts 24% OG component.

Previous models also predicted an unreasonably high abundance of orange glass in the soils from the South Massif. The model of *Rhodes et al.* (1974) indicated 6-7% OG component in soils from stations 2 and 2A, yet only 2-3% HT component. More extreme, the model of *Laul et al.* (1981) indicated nearly 12% OG component in soil 72501 (a typical station 2 soil) but ~4% HT component. Petrographic data suggest that the abundance of orange glass is small [2.9 ± 1.6% orange and black glass and 3.8 ± 2.1% mare basalt, mean and standard deviation in the nonagglutinate portion of the 90-150-μm fractions of six soils from stations 2 and 2A (*Heiken and McKay,* 1974); but see caveat, section 4.2]. Therefore, the model results obtained here, that the soils from stations 2 and 2A average only 3.5 ± 1.2% OG component and 2.1 ± 1.1% MB component, are more reasonable. The ratio of orange glass

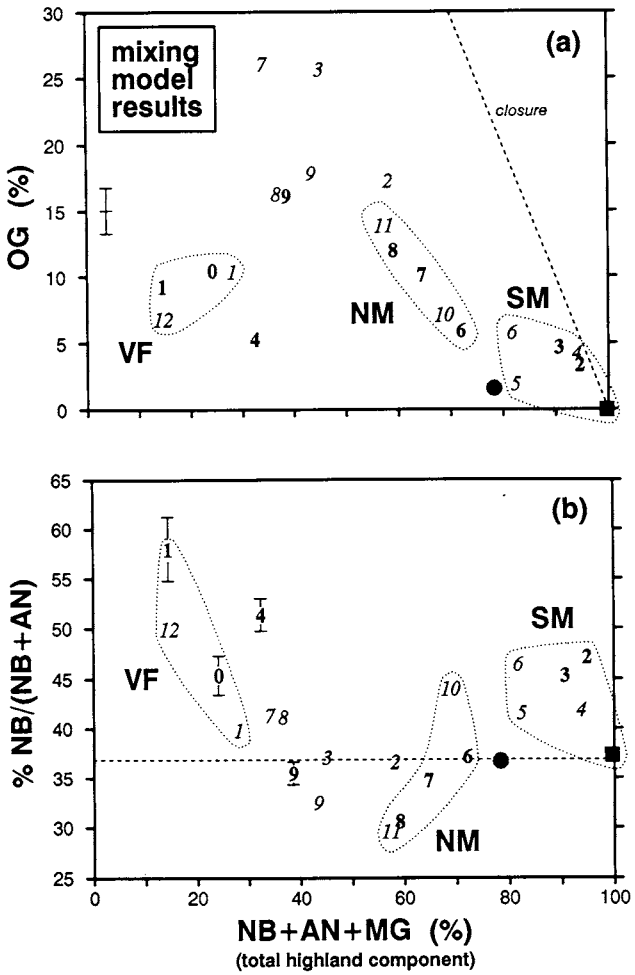

Fig. 8. Some mixing model results as a function of abundance of total highland component, NB + AN + MG (noritic breccia, anorthositic norite, and high-*Mg'* components). The sample-station key is the same as in Fig. 2. VF = valley-floor soils, SM = South Massif soils, and NM = North Massif soils. Model results for the station 5 soils are unreliable (section 4.9) and are not plotted here. **(a)** The orange glass (OG) component is most prevalent in soil from LRV stops 7 and 3 but is considerably less prevalent in the gray soil from station 4. A typical 1σ estimate of model uncertainty is shown. **(b)** Both the 73131 regolith breccia (square) and the ropy glass particles from station 4 (circle) have the same abundance ratio NB/(NB + AN), whereas South Massif soils tend to have relatively more NB component and North Massif soils tend to have about the same or less. Model uncertainty in the ratio NB/(NB + AN) decreases with total highland components; some typical values are shown. The high NB/(NB + AN) ratio for the valley-floor soils indicates that the nonmare component of these soils derives from beneath the basalt flows, not from the massifs.

to mare basalt (OG/MB) in the South Massif soils (~1 or greater) is high compared to soils from the valley floor (0.1-0.2 at the LM area to 0.9 at LRV-3). As the light-mantle avalanche was a relatively recent event (section 5.2), there is no mechanism for so effectively concentrating orange glass relative to crystalline mare basalt in these highland soils since the light-mantle avalanche. This suggests that much of the orange glass in the South Massif soils is ash deposited during the eruption of the pyroclastics, not regolith from the valley floor redistributed by subsequent impacts.

The model predicts that the greatest concentration of OG component occurs in soils from LRV stops 3 and 7 (>25%; Fig. 8a). This result is perhaps expected as each stop is within 2 km of station 4 (Fig. 2) where orange glass was found in concentrated form (>95% in 74220). LRV-6 is also within 2 km of station 4, but the model predicts only 6% OG component. This is because the LRV-6 soil (74121) consists mainly of highland material associated with the light mantle deposit, whereas the soils from LRV-3 and LRV-7 contain less highland material than any soils from the light-mantle area except those from station 4. A surprising model result is that the gray soil from station 4 has a low abundance of the OG component (5.3 ± 1.8%), lower than that of any other soil from the valley floor, even though the orange-glass sample (74220) was taken from the same trench as the gray soil. A possible reason for this apparent anomaly is discussed in section 5.2.

The abundance of OG component decreases systematically from east to west in the North Massif soils (Figs. 2 and 8a). This is an effect of closure and of the increase in the abundance of highland components in the same direction.

4.12. Relative Proportions of Highland Components

4.12.1. Massif soils. One of the principal observations of *Rhodes et al.* (1974) was that the ratio of noritic impact-melt breccia to "anorthositic gabbro" components was greater in soils from the South Massif than from the North Massif. This model result, which is reproduced by our model (Fig. 8b), is a direct consequence of the higher concentrations of ITEs in the South Massif soils (Figs. 3 and 5). The light-mantle deposit is derived from the upper slopes of the South Massif whereas nonmare material in the soils of the North Massif and Sculptured Hills is derived primarily from the lower slopes. This led *Rhodes et al.* (1974) to hypothesize that the massifs were essentially similar to each other but that they were stratified, with the NB component being more prevalent at higher elevations. Such stratification is the likely consequence of deposition of mafic, ITE-rich impact melt upon anorthositic crustal material during a basin-forming impact (Serenitatis). New data presented here allow further consideration of the hypothesis of *Rhodes et al.* (1974).

Among the South Massif stations (2, 3, LRV-4, LRV-5, and LRV-6), the NB/(NB + AN) component ratio is relatively constant at 42-47% (Fig. 8b). The lowest NB/(NB + AN) ratio among South Massif samples occurs in regolith breccia 73131 (37%). This suggests that the composition of other South Massif soils can be reproduced by mixing the NB component and 73131, with additional minor amounts of the MB, OG, and KB components. We have tested this alternate model, which includes no explicit AN or AG component, and it accounts as well for the composition of South Massif soils as does the model of Table 5. (Mathematically, it must because the AN component is a calculated composition based on 73131 and the NB component.) In this model, the abundance of NB component (in excess of that contributed by the 73131 component) ranges from 6% at LRV-5 to 14% at station 2.

These observations are consistent with the hypothesis of *Rhodes et al.* (1974) if 73131 represents regolith from the lower slopes of the South Massif with addition of variable amounts of ITE-rich, noritic impact-melt breccia from the upper slopes to account for the other soils.

Although 73131 almost certainly derives from the South Massif, soils from the North Massif (stations 6 and 7) have a similar NB/(NB + AN) ratio (Fig. 8b) (but they also contain a component of high-*Mg'* lithologies not seen in the South Massif soils). This is also consistent with the hypothesis of *Rhodes et al.* (1974). Boulders sampled at station 6 are believed to have come from about a third of the way up the North Massif (*Wolfe et al.,* 1981). These boulders are composed predominantly of ITE-rich, noritic impact-melt [e.g., samples 76015 and 76315 of *Rhodes et al.* (1974)]. However, the abundance of NB component in the station 6 soils is only 21%, compared to 39% and 42% for the soils from stations 2A and 2 (Table 5). Two of the station 6 soils analyzed here with the highest ITE concentrations were taken near one of these ITE-rich boulders (section 3.1.2), but the ITE concentrations in these two samples correspond to an average of only 3% NB component in excess of that in the other soils. Thus, the station 6 soils do not obtain a significant fraction of their material from the upper slopes of the North Massif.

Among North Massif soils, only previously unstudied soil 76131 from LRV-10 has a high NB/(NB + AN) ratio, similar to that of the South Massif soils (Fig. 8b). This sample was collected near 6-m-high "Turning Point" rock at the contact between the valley floor and the North Massif; it probably contains material filleted from a smaller ancillary boulder (see Fig. 141 of *Wolfe et al.,* 1981). A small rock (76135) collected with soil 76131 is a typical noritic impact-melt breccia (R. L. Korotev, unpublished data, 1991). The composition of 76131 can be modeled well as a mixture of 84% station 6 soil, 7% HT component, and 9% NB component; the NB component presumably was derived from the boulder. Although *Wolfe et al.* (1981) do not speculate on the origin of Turning Point rock and related boulders, it is likely that they derive from the North Massif, as they are located at the bottom of the hill. Perhaps the greater component of noritic breccia in 76131 compared to those from station 6 indicates that Turning Point rock and nearby boulders have been located at their present position longer than the station 6 boulders and thus are more highly degraded.

In summary, the major difference between the soils from the two massifs is that the light mantle deposit at the South Massif has a large component of regolith that developed high on the massif, and this regolith has a large component of noritic impact-melt breccia. During the light-mantle avalanche, the noritic-breccia-rich soil mixed incompletely with regolith at the base of the massif, and that regolith has a lower abundance of noritic breccia. This highland regolith covered a regolith consisting largely of mare basalt and orange pyroclastic glass, and the extent of impact mixing since the avalanche has not been large. At the North Massif, most of the regolith was derived from the local materials at the interface between the valley floor and highlands (*Rhodes et al.,* 1974; *Wolfe et al.,* 1981). Material that was derived from high on the North Massif still exists mostly as large boulders, not as regolith fines, because the boulders were emplaced at their present position relatively recently, 22 ± 1 Ma ago (*Crozaz et al.,* 1974).

Soil from the North Massif stations also contain high-*Mg'* components (MG), modeled here as troctolite and norite; 10-25% of the highland material in these soils is MG component. No similar component is required for mass balance in the South Massif soils. When the abundances of the three highland components of the North Massif soils (NB + AN + MG) are normalized to 100%, there is no correlation between the model-predicted abundances of MG and NB components (R^2 = 0.02). However, MG component weakly anticorrelates with AN component (R^2 = 0.66) because the fraction of NB component remains relatively constant (27-38% of total). The MG component is most similar in composition to the AN component (Fig. 5), but more mafic and magnesian. The anticorrelation reiterates the point made earlier (section 4.4) that the feldspathic, ITE-poor lithologies of the regolith are highly variable in Al_2O_3/(FeO + MgO) and *Mg'*. Although modeled here as plutonic troctolite and norite, the MG component also represents brecciated equivalents of these rocks [e.g., high-*Mg'* granulitic breccias; *Lindstrom and Lindstrom* (1986)].

4.12.2. Valley-floor soils. Other than the anomalous station 5 soils (section 4.10), the soils containing the largest amount of mare material (basalt and pyroclastic glass) are those from stations LM/ALSEP (i.e., 0), 1, and LRV-12 located near the center of the valley floor (Fig. 2). Model results indicate that although the abundance of nonmare material is small (NB + AN = 15-24%), the NB/(NB + AN) ratio is as high or higher at these three stations than at the South Massif and is much higher than at stations nearer the North Massif (Fig. 8b). Such high ratios are not expected if the highland material in the valley-floor soils derives from impacts into the nearest exposed highlands, namely, the lower slopes of the massifs. Instead, the model results show that over distances as small as a few kilometers, lateral movement of material is not an effective transport mechanism and that most of the highland material in the valley-floor soil derives from vertical mixing of material from below the basalt flows of the valley floor (*Rhodes,* 1977). The Taurus-Littrow valley was formed from a down-fallen block associated with high-angle faulting during formation of the Serenitatis Basin (*Wolfe et al.,* 1981, Fig. 242). Assuming that the stratigraphic model of *Rhodes et al.* (1974) is valid, then the highland material immediately below the valley floor is similar to material that is (or at one time was) at the top of the massifs, i.e., it has a high NB/(NB + AN) ratio, perhaps higher than that of the South Massif soils. The high NB/(NB + AN) ratios of the highland component of the valley-floor soils indicate that mixing of material over vertical distances of 1-2 km (the thickness of the basalt at the landing site; *Wolfe et al.,* 1981) is more effective than mixing over lateral distances of 4-10 km.

4.12.3. Gray soil from station 4. The model predicts a high NB/(NB + AN) ratio for the gray soil (samples 74241 and 74261) from station 4, higher than that of any of the South Massif soils (Fig. 8b). The high abundance of NB component in this soil effectively accounts for the high concentrations of Sm (Fig. 3) and other ITEs (except Na, see section 4.9) in the gray soil compared to other similarly mafic soils. The gray soil is petrographically unusual in containing a high proportion

of "low-grade breccia with colorless glass matrices" (5-13% in the 90-150-μm grain-size fraction; *Heiken and McKay,* 1974). These breccias may be the carriers of the NB component in the gray soil because soil from stations 2 and 3 are also rich in both low-grade breccias (*Heiken and McKay,* 1974) and NB component (Table 5 and section 5.2).

4.13. Siderophile Elements

Concentrations of siderophile elements Ni, Ir, and Au are low in Apollo 17 soils compared to Apollo 16 soils because the noritic impact-melt breccias from which the Apollo 16 soils are in part derived have high concentrations of Fe-Ni metal of meteoritic origin compared to the Apollo 17 noritic impact-melt breccias (*Korotev,* 1987a,b). Concentrations of Ni, Ir, and Au are near the detection limits of INAA for most of the samples studied here and have correspondingly high relative uncertainties. The CI component was included to account for siderophile-element concentrations in the few high-Ni samples and to help with the mass balance for Co, which is determined precisely but which is both a lithophile and siderophile element. The NB and AN components, whose compositions were derived from samples of polymict breccias, and the OG component, whose composition was derived from a regolith sample (74220), each contain Ni, Ir, and Au from meteoritic sources. (We have assumed that the mare basalt components have effectively zero concentrations of Ni, Ir, and Au.) Therefore, the CI component of the model accounts only for the excess concentration of siderophile elements above those contributed by the model components. This is why the model abundances of CI component (Table 5) are low compared to the value of 1.76% "extralunar component" estimated by *Baedecker et al.* (1974) for mature Apollo 17 soils. The "extralunar component" represents both ancient, breccia-forming meteorites and micrometeorites such as those striking the surface today; the CI component of our model more closely represents the micrometeorite component.

Split 76031A contains a fragment of meteoritic metal. The sample contains high concentrations of siderophile elements compared to other samples (section 3.1.3). The siderophile-element enrichment can be explained reasonably well by the mass-balance model with 5.4% CI component, compared to 1.2% for the mean of all station 6 soils. However, concentrations of siderophile elements in the best-fit mixture do not match observed concentrations well. By comparing concentrations of siderophile elements in 76031A to mean concentrations in the other station 6 soils, ratios of siderophile elements to Ni in the "excess" component can be calculated. This yields the following CI-normalized ratios: Fe/Ni = 0.8 ± 0.2, Co/Ni = 1.6 ± 0.2, Ir/Ni = 0.71 ± 0.16, and Au/Ni = 1.2 ± 0.4 (±95% confidence). The Co/Ni ratio is similar to that of metal fragments observed petrographically in Apollo 17 soils (*Goldstein et al.,* 1974) and the other ratios are similar to those of metal from Apollo 16 rocks and soil (*Korotev,* 1987b). The siderophile-element-bearing component contains little or no silicate material because the split does not have high ratios of Na/Sm and Cr/Sc compared to other station 6 soils; these ratios would be anomalously high if the split contains a 4.2% (5.4% minus 1.2%) excess of any type of chondritic material.

Because of the poor analytical precision of the Ni, Ir, and Au data and the large variability in siderophile-element concentrations among different splits of a soil from a given sampling station, *differences* predicted by the model in the abundance of CI component between different stations (Table 5) have no significance.

5. ROPY GLASS PARTICLES AND GRAY SOIL FROM STATION 4

5.1. Ropy Glass Particles (RGPs)

Glassy particles with ropy morphologies are found in many lunar soils, although they are not common. They typically appear as elongated droplets with twisted or fluted surfaces and coatings of fine-grained particulate debris (*Fruland et al.,* 1977). Ropy glasses are believed to be melts formed and dynamically shaped during major impacts (*McKay et al.,* 1971; *Meyer et al.,* 1971; *Cavarretta et al.,* 1972). The gray soil from station 4 on the rim of Shorty Crater contains a high proportion (10-20%) of ropy glass particles (RGPs) (*Heiken and McKay,* 1974). Because material ejected from Tycho Crater in the southern highlands is believed to have reached the Apollo 17 site (*Arvidson et al.,* 1976), *Fruland et al.* (1977) studied the RGPs from station 4 and explored the exciting possibility that the ropy glass might be ejecta from Tycho. They observed that although the station 4 soil contains primarily mare-derived material, the interior glassy portions of the RGPs had a nonmare major-element composition that was uniform from particle to particle. The glass composition was intermediate to those of the noritic breccia and anorthositic gabbro components of *Rhodes et al.* (1974) (Fig. 5), suggesting that the RGPs might be the product of an impact into the local highlands. However, *Fruland et al.* (1977) noted that rocks and soil of generally similar bulk composition occur at other highland sites. Therefore, the major-element data alone were not sufficient to exclude the possibility that the station 4 RGPs were from some exotic location in the highlands.

Results of INAA for six individual RGPs from station 4 soil 74242 (i.e., 1-2-mm grain-size fraction) are presented in Table 7. Results of EMPA for major elements on a fused bead prepared from grinding together the six particles after INAA are presented in Table 8 (column 1). Because both analytical techniques provide bulk analyses, the results represent the interior glass as well as any entrained clasts and surface-coating material. Variation in clast composition and number leads to most of the variation in composition among the six RGPs (Table 7). Compared to the colorless interior glass (Table 8, column 3), the bulk particles are poorer in Al and Ca and richer in Fe, Cr, and particularly Ti, indicating that the nonglassy components are primarily of mare origin.

The mass-balance model, which accounts for the compositions of <1-mm fines, also accounts well for the bulk composition of the RGPs (χ^2/ν = 3.8, a reasonable value considering that the composition modeled is based on <17 mg of material). The model suggests that the RGPs are a mixture of 29% NB, 50% AN, 20% MB, and 2% OG components (Tables 5 and 7). This OG/MB ratio (0.1) is at the low end of the range observed in <1-mm soils and is essentially the

TABLE 8. (1) Average compositions of ropy glass particles (RGPs) from 74242 and comparison with (2) nonmare portion calculated from mixing model, (3) composition of "colorless interior glass" (*Fruland et al.*, 1977), and (4) regolith breccia 73131, which is assumed to have no mare components.

Sample:		Station 4 RGPs			Reg. Brx.
		74242 Bulk	74242 Nonmare	Interior Glass	73131 Nonmare
Source:		Analysis	Model	Analysis	Analysis
Column:		(1)	(2)	(3)	(4)
SiO_2	%	44.5	45.8	45.4	45.0
TiO_2	%	2.8	0.52	0.48	0.92
Al_2O_3	%	20.0	23.0	23.1	22.55
FeO	%	9.69	7.16	6.11	7.13
MgO	%	9.24	9.26	9.24	9.36
CaO	%	12.3	12.7	13.61	13.45
Na_2O	%	0.411	0.421	0.29	0.434
Sc	μg/g	28.3	14.9	n.a.	14.8
Cr	μg/g	1700	1210	1160	1260
Co	μg/g	21.8	21.1	n.a.	22.9
Ni	μg/g	120	150	n.a.	190
Sr	μg/g	156	154	n.a.	146
Zr	μg/g	216	224	n.a.	200
Ba	μg/g	156	180	n.a.	178
La	μg/g	12.3	14.2	n.a.	14.7
Ce	μg/g	33.7	37.9	n.a.	38.4
Sm	μg/g	7.22	7.03	n.a.	6.89
Eu	μg/g	1.37	1.29	n.a.	1.18
Tb	μg/g	1.58	1.48	n.a.	1.33
Yb	μg/g	5.74	5.26	n.a.	5.08
Lu	μg/g	0.803	0.730	n.a.	0.700
Hf	μg/g	5.71	5.31	n.a.	5.31
Ta	μg/g	0.82	0.60	n.a.	0.67
Ir	ng/g	7.0	8.9	n.a.	5.8
Au	ng/g	2.9	3.7	n.a.	2.6
Th	μg/g	2.02	2.47	n.a.	2.53
U	μg/g	0.58	0.70	n.a.	0.74
Model results					
MB	%	19.9	0	—	0.0
OG	%	1.6	0	—	0.0
NB	%	28.7	36.7	—	37.1
AN	%	49.6	63.3	—	62.6

(1) SiO_2, TiO_2, Al_2O_3, FeO, MgO, and CaO data from EMPA of a fused bead prepared from grinding together six RGPs (Table A2); other data are mass-weighted mean concentrations from INAA of six individual RGPs (Table 7).

(2) Results of algebraically removing MB and OG components (Table 4) in proportions predicted by mixing model (Table 5) from data of column (1) and renormalizing.

(3) EMPA; trace elements were not analyzed (n.a.) (*Fruland et al.*, 1977).

(4) Composition of 73131 regolith breccia (Table 2).

mixture of model components (section 4.4). Petrographically, the gray soil contains high abundances of RGPs and low-grade breccias (section 4.1.1; *Heiken and McKay*, 1974). Results of the mass-balance model suggest that the abundance of orange glass is lower in the gray soil than that for any other similarly mafic soil (5.3% OG component; station 4, Table 5 and Fig. 8a). The model also suggests that the highland components have a relatively high proportion of ITE-rich noritic breccia [high NB/(NB + AN); Fig. 8b]. The carrier of the NB component may be the "low-grade breccias" of *Heiken and McKay* (1974).

The gray soil, like the orange soil, is an old soil recently excavated by the Shorty Crater impact (*Wolfe et al.*, 1981). Exposure ages for the orange soil (74220) based on cosmogenic nuclides indicate that Shorty Crater was formed within the last 30 Ma (*Hunecke et al.*, 1973; *Husain and Schaeffer*, 1973). Therefore, the highland material in the gray soil is not derived from the light-mantle avalanche and we should not necessarily expect the NB/(NB + AN) ratio to be the same as in soils from nearby LRV-5 and LRV-6, which contain high proportions of light mantle material.

All three station 4 soils (74220, 74241, and 74261) are very immature, indicating that they have had little surface exposure (*McKay et al.*, 1974; *Morris et al.*, 1983). This and other observations led *Heiken et al.* (1974) to suggest that the orange glass pyroclastics were buried shortly after their eruption by "large basalt flows or a large impact blanket." The eruption occurred at least 3.5 Ga ago (see summary in *Heiken et al.*, 1974) and the 74220 material was buried until the Shorty Crater impactor penetrated the light mantle. The present proximity of the orange and gray soils at station 4 suggests that they may have been stratigraphically adjacent prior to excavation by the Shorty Crater impact. However, the gray soil cannot have received its volatiles directly from spatial proximity to the volcanic vent(s) that erupted the orange glass, nor can orange glass be the carrier of the volatiles in the gray soil because the abundance of orange glass in the gray soil is too low (5.3%). We consider it more likely that the volatile enrichments in the gray soil result from remobilization and condensation of volatiles previously associated with the orange glass as a result of the proximity of the gray soil and the orange soil. Perhaps a warm deposit of pyroclastics was buried by a cooler deposit of gray soil and the volatiles migrated upward.

What is the source of the highland material in the gray soil? Some of the highland material is in the form of RGPs, which are probably impact products transported laterally to the valley floor (section 5.1). RGPs have a lower NB/(NB + AN) ratio (0.37) than the bulk soil (0.51, Fig. 8b), therefore, the remaining highland material of the gray soil must have a high NB/(NB + AN) ratio (>0.51). We estimate that ratio to be 0.60, assuming that abundance of RGPs in the gray soil is 16% (90-150-μm grain-size fraction; *Heiken and McKay*, 1974). This is similar to the value obtained at station 1 on the valley floor (Fig. 8b). As at station 1, the highland material in the gray soil (that which is not RGPs) probably derives from beneath the valley floor, not from the surrounding massifs. It is likely that at the time the basalt flows first filled the valley, a highland regolith existed on the valley floor (e.g, *McKay et al.*, 1986) and that regolith was rich in NB component. The gray soil may be regolith that formed by mixing of basalt and underlying highland regolith at a time when the basalt flows were thinner and before substantial addition of the pyroclastics.

6. SUMMARY AND CONCLUSIONS

Variation in the proportions of six chemical components accounts for most of the compositional variation in Apollo 17 soils. Each of the chemical components is represented by lithologic components observed in the regolith. Three of the

chemical components are of mare origin: (1) high-Ti mare basalt, (2) VLT basalt, and (3) pyroclastic orange glass; three are of highland origin: (4) noritic impact-melt breccia, (5) anorthositic norite breccia, and (6) high-Mg/Fe troctolites and norites. Results of a six-component mass-balance model indicate that VLT basalt is a minor component, composing only about 8% of the total basalt component on average. Orange glass is a less-abundant component of the Apollo 17 regolith than estimated in some previous models but composes up to 26% of some soils. The troctolite/norite component is only important in soils from the North Massif and reaches a maximum of about 15% in the soils from station 6 (the exact abundance depends upon assumptions regarding the relative proportions of troctolite and norite and how anorthositic these lithologies are on the average). This component is probably carried by plutonic cumulates of the Mg-suite as well as their brecciated derivatives (granulitic and impact melt breccias).

Regolith breccia 73131 is the only regolith sample from Apollo 17 that is virtually devoid of mare material. The ratio of noritic impact-melt breccia to anorthositic norite components is similar in 73131 and soils from stations 6 and 7 at the North Massif, but is less than that of soils from the South Massif, which are thought to derive mainly from the upper slopes of the massif. Because the highland components of the North Massif soils are thought to derive mainly from the lower slope of the massif, by analogy we may suspect that 73131 derives from the lower slopes of the South Massif. For other South Massif soils, which are thought to derive from the upper slopes of the massif, the compositions can be reproduced by mixing 73131 with noritic impact-melt breccia and minor amounts of mare material. This observation is reasonable in terms of the hypothesis of *Rhodes et al.* (1974) that the upper slopes of the massifs contain a higher proportion of noritic impact-melt breccia than the lower slopes. The only soil sample from the North Massif with a high proportion of noritic impact-melt breccia compared to anorthositic norite is from LRV stop 10 at Turning Point rock. The excess noritic breccia component may derive from a nearby noritic boulder that probably originated from high on the massif. The nonmare component of soils from the center of the valley floor probably derives largely from beneath the basalt flows, not from the massifs, because these soils also have high ratios of noritic breccia to anorthositic norite.

Ropy glass particles from station 4 have a glassy matrix with the same general composition as regolith breccia 73131 and a bulk composition consistent with admixture of local basalt as clasts or surface coating. They are most probably of local origin and not ejecta from Tycho. The gray soil in which the ropy glass particles were found is unusual in containing high concentrations of ITEs compared to other similarly mafic soils. The high concentrations can be attributed to a high abundance of noritic impact-melt breccia. The source of this breccia component is not the light mantle avalanche, but probably old highland regolith below the valley floor.

The two soils from station 5 (75061 and 75081) are the most mafic, indicating that they have the largest component of mare basalt. However, their compositions are poorly fit by the mass-balance model. They apparently contain an unidentified component not evident in other valley-floor soils. Two other valley-floor soils (71041 and 71061 from station 1) are also not well fit by the model and appear to contain a basalt component different from typical high-Ti mare basalt, one with higher concentrations of Na, Eu, and ITEs. Each of these four soils is more immature than most valley-floor soils and consists in part of fresh crater ejecta.

A given sample of lunar soil is composed of a large number of compositionally distinct, lithologic components and the number of those components exceeds the number of chemical components modeled here and the number that can be reasonably constrained using compositional mass-balance models. Thus, the six-component model does not achieve ideal agreement for every sample. In addition to the major model components, poor fits to data for some samples imply the presence of (1) mineral grains (e.g., whitlockite, zircon) in excess of those representative of modal proportions in the rocks from which they derive, (2) other types of mare basalt (in the station 5 and two station 1 soils), (3) KREEP basalt (at station 2), (4) meteoritic material not represented by the CI component (in 76031A), and (5) a Na-rich volatile component (in the gray soil from station 4). However, a small number of components with fixed compositions succeeds in accounting reasonably well for the composition of representative soils because certain suites of subcomponents occur in relatively constant proportion as a result of different episodes of impact mixing (*Korotev,* 1987c). For example, noritic impact-melt breccias derive from a variety of older crustal components that were well mixed during formation of the breccias and prior to their incorporation into the regolith. The relative proportions of different basalt types is probably not highly variable among mature (= well-mixed) valley-floor soils because any stratification has been partially erased by the regolith-forming process. The anorthositic-norite component of the model represents the average composition of lithologies with a range of compositions; however, in different samples of soil the relative proportions of these lithologies are not so highly variable that they each need be represented by a different component in the model. Compositional variation among soil samples usually reflects the last major mixing events, and those events often involve mixing of polymict regolith with other polymict regolith.

APPENDIX

TABLE A1. Results of INAA of ~50-mg samples of Apollo 17 <1-mm fines.

	Station	Lab id.	Na_2O %	Sc μg/g	Cr μg/g	FeO %	Co μg/g	Ni μg/g	Sr μg/g	Zr μg/g	Ba μg/g
70161	ALSEP	253.34	0.383	60.7	3080	17.0	33.2	180	170	150	100
70181	ALSEP	253.20	0.389	59.5	3060	16.6	33.7	150	270	220	90
70251	SEP	253.43	0.402	59.0	3000	16.7	34.5	180	190	200	100
70271	SEP	253.32	0.395	61.7	2970	16.7	35.5	160	140	230	100
70311	LRV-12	253.22	0.374	65.7	3160	17.5	33.9	160	190	260	110
70321	LRV-12	253.28	0.377	66.8	3140	17.1	28.4	90	160	280	80
71041	1	253.29	0.408	66.7	3190	18.0	30.1	80	150	290	110
71061 A	1	253.14	0.423	64.7	3110	18.0	32.7	70	210	230	150
71061 B	1	258.11	0.411	63.1	3390	18.3	34.4	90	100	270	74
71131	1	255.72	0.374	66.5	3210	17.9	34.4	180	100	210	100
71151	1	253.02	0.376	66.7	3100	17.6	30.7	100	150	170	110
71501 A	1	253.19	0.380	66.6	3130	17.8	32.1	140	210	230	110
71501 B	1	258.06	0.384	66.4	3120	17.4	30.3	140	180	230	81
72131	LRV-1	253.07	0.396	58.4	2960	16.5	33.4	180	150	180	96
72150	LRV-3	253.44	0.398	43.4	2810	14.9	40.9	250	180	280	128
72161	LRV-3	253.33	0.397	41.2	2900	14.9	44.7	320	140	190	119
72221 A	2	205.61	0.463	21.0	1730	8.89	28.9	237	152	250	204
72221 B	2	213.59	0.456	18.9	1540	8.68	30.8	289	142	260	200
72241 A	2	205.62	0.472	19.7	1620	8.84	27.5	214	161	310	224
72241 B	2	213.60	0.466	19.0	1610	8.59	26.2	212	200	250	208
72261 A	2	205.63	0.452	18.9	1560	8.55	29.5	277	167	290	239
72261 B	2	213.61	0.427	17.8	1490	8.24	27.6	252	165	270	195
72431 A	2	205.64	0.464	19.6	1620	8.92	28.9	242	158	270	209
72431 B	2	213.62	0.464	18.6	1509	8.55	25.6	222	159	240	196
72701 A	2	213.5X	0.456	19.1	1570	8.85	34.2	341	158	250	194
72701 B	2	253.21	0.452	18.7	1577	9.04	39.0	350	181	280	193
73131 A	LRV-4=2A	205.60	0.437	14.5	1240	6.87	20.3	157	147	210	190
73131 B	LRV-4=2A	213.63	0.431	15.1	1290	7.18	25.5	227	146	190	167
73151 A	LRV-4=2A	205.65	0.442	18.8	1580	8.60	32.0	249	154	240	188
73151 B	LRV-4=2A	213.64	0.420	18.7	1490	8.38	30.7	317	173	210	176
73211 A	3	205.66	0.439	20.6	1640	8.93	28.5	203	163	230	185
73211 B	3	213.65	0.442	19.6	1500	8.68	28.0	258	156	270	198
74111	LRV-5	253.27	0.434	24.7	1782	9.92	30.5	242	178	250	166
74220	4	253.N6	0.366	48.3	4650	22.2	61.5	113	235	175	78
74241 A	4	253.39	0.457	61.0	2780	16.2	26.3	90	170	270	120
74241 B	4	253.40	0.471	57.3	2800	15.3	26.7	140	210	200	109
74261	4	253.23	0.476	53.9	2950	15.6	30.2	120	140	250	127
75061 A	5	253.36	0.344	75.2	3480	18.0	26.3	<100	130	250	80
75061 B	5	258.05	0.364	69.9	3280	17.9	27.8	100	210	330	105
75081 A	5	258.01	0.372	66.9	3240	17.8	29.9	50	170	230	100
75081 B	5	258.02	0.374	65.9	3190	17.5	31.2	150	210	180	108
75111	LRV-7	253.15	0.419	49.3	3060	16.2	38.3	160	200	220	123
75121	LRV-8	253.16	0.398	49.9	2900	16.0	38.2	220	210	130	124
76031 A	6	253.35	0.373	32.1	2036	12.0	88.7	990	150	170	130
76031 B	6	253.48	0.381	29.4	1973	10.9	33.6	220	170	250	126
76121	LRV-9	253.25	0.405	43.7	2640	14.5	35.3	230	140	230	126
76131	LRV-10	253.06	0.415	31.6	2017	11.3	29.3	200	190	230	144
76221 A	6	253.24	0.383	28.9	1917	10.9	40.1	340	166	170	123
76221 B	6	253.47	0.383	27.0	1888	10.3	31.8	230	160	170	132
76241 A	6	253.18	0.415	29.3	1890	10.4	27.1	170	160	200	121
76241 B	6	258.07	0.422	27.6	1870	10.3	29.0	230	160	190	132
76261 A	6	253.30	0.427	27.1	1794	10.4	34.0	220	185	200	158
76261 B	6	258.08	0.403	28.9	1930	10.7	29.4	200	150	230	124
76281 A	6	253.04	0.388	31.2	2031	11.0	29.9	170	160	160	131
76281 B	6	258.09	0.399	31.4	2020	11.2	29.9	190	180	150	116
76321 A	6	258.03	0.425	26.6	1810	10.1	28.2	180	150	240	149
76321 B	6	258.04	0.416	27.0	1820	10.3	32.1	230	180	210	141
76501 A	6	196.43	0.379	29.2	1980	10.7	31.0	210	130	170	114
76501 B	6	253.09	0.375	27.5	1848	10.5	35.0	260	164	160	108
77511	7	253.37	0.396	32.1	2160	11.4	31.3	240	130	210	127
77531	7	253.38	0.402	34.3	2170	11.9	32.1	260	160	200	136
78121	LRV-11	253.08	0.410	37.0	2360	12.8	34.6	310	150	250	107
78221 A	8	196.42	0.376	34.6	2370	12.0	35.9	280	140	180	118
78221 B	8	253.05	0.378	34.3	2270	11.9	37.0	230	170	180	106
78231	8	253.17	0.377	34.9	2300	12.0	35.5	260	170	200	131
78250	8	253.13	0.375	37.1	2410	12.5	38.2	180	140	200	108
78421 A	8	253.45	0.376	36.7	2270	12.4	51.4	240	170	170	104
78421 B	8	258.10	0.392	37.4	2390	12.6	36.9	240	180	200	97
78441	8	253.11	0.386	35.1	2210	12.1	34.6	230	180	210	107
78461	8	253.42	0.381	34.8	2230	11.9	31.7	230	220	190	132
78481	8	253.41	0.376	35.8	2310	12.2	36.9	340	140	150	109
78501	8	255.74	0.387	42.3	2480	13.4	33.9	210	170	220	120
79121	9	253.12	0.418	49.3	2780	15.7	43.2	310	210	230	120
79221	9	253.01	0.394	49.9	2780	15.5	36.7	240	200	2140	94
79241	9	253.10	0.422	50.0	2870	15.6	34.8	220	160	240	93
79261	9	253.03	0.395	52.4	2900	15.8	35.0	180	160	160	99
79511	9	253.31	0.421	49.1	2840	15.4	34.4	200	240	160	107
±			0.005	0.5	30	0.2	0.4	50	50	50	15

TABLE A1. (continued).

	La µg/g	Ce µg/g	Nd µg/g	Sm µg/g	Eu µg/g	Tb µg/g	Yb µg/g	Lu µg/g	Hf µg/g	Ta µg/g	Ir ng/g	Au ng/g	Th µg/g	U µg/g
70161	7.89	23.4	17	8.11	1.74	2.03	7.20	1.01	7.12	1.25	6.	4.	0.84	0.18
70181	8.22	24.9	25	8.02	1.67	1.96	6.97	0.94	6.66	1.10	<5.	<7.	0.90	0.50
70251	8.26	23.7	21	8.17	1.76	2.03	7.22	0.99	6.80	1.21	6.	5.5	1.01	0.24
70271	7.74	23.3	24	8.12	1.70	1.94	7.28	1.03	6.78	1.17	7.	4.	0.78	0.30
70311	7.17	22.2	24	8.02	1.63	1.95	7.26	1.05	7.27	1.36	<8.	<9.	0.69	<0.5
70321	7.14	22.5	22	7.89	1.68	1.99	7.38	1.03	7.20	1.20	6.	<8.	0.67	0.20
71041	7.65	23.3	18	8.64	1.84	2.19	7.77	1.08	7.48	1.33	9.	<6.	0.64	0.22
71061 A	8.04	23.6	19	8.59	1.77	2.08	7.71	1.06	7.58	1.43	<5.	<10.	0.87	0.30
71061 B	7.13	21.6	17	8.09	1.71	1.98	7.11	0.995	7.17	1.22	<12.	<7.	0.63	<0.4
71131	7.33	22.4	16	8.08	1.62	2.12	7.36	1.04	7.38	1.33	n.a.	<6.	0.80	<0.6
71151	7.26	23.2	17	8.15	1.67	2.06	7.39	1.03	6.97	1.36	10.	5.	0.69	0.19
71501 A	7.36	23.4	23	8.10	1.69	1.95	7.50	1.04	7.15	1.27	7.	4.	0.74	0.20
71501 B	7.30	21.3	18	7.88	1.66	1.97	7.36	1.03	7.05	1.28	<3.	5.	0.68	<1.0
72131	8.18	24.3	21	7.76	1.62	1.85	6.65	0.920	6.60	1.20	5.	6.	0.93	0.36
72150	9.46	27.0	20	7.07	1.44	1.67	5.73	0.807	6.01	0.94	9.5	4.3	1.21	0.46
72161	9.80	28.4	22	7.12	1.44	1.61	5.61	0.796	5.96	0.87	12.5	5.2	1.41	0.32
72221 A	18.0	47.4	31	8.73	1.34	1.72	6.56	0.912	6.76	0.86	8.0	3.6	3.60	0.79
72221 B	17.8	45.8	27	8.51	1.32	1.63	6.21	0.855	6.75	0.89	9.0	3.2	3.25	0.84
72241 A	19.7	51.5	34	9.36	1.38	1.87	7.05	0.963	7.66	0.89	5.7	2.8	3.20	0.84
72241 B	19.0	49.6	30	9.04	1.35	1.74	6.61	0.931	7.10	0.83	5.5	2.9	3.26	1.00
72261 A	19.0	50.1	31	9.19	1.33	1.76	6.67	0.900	6.65	0.84	9.2	3.6	3.20	0.81
72261 B	18.8	49.4	30	8.76	1.29	1.70	6.40	0.871	6.90	0.83	9.0	2.6	3.04	0.59
72431 A	17.3	46.0	30	8.40	1.36	1.62	6.26	0.857	6.75	0.83	8.3	2.9	2.90	0.75
72431 B	18.2	47.9	30	8.65	1.35	1.68	6.50	0.894	6.69	0.82	6.7	4.6	3.30	0.78
72701 A	17.8	46.8	28	8.51	1.34	1.65	6.16	0.853	6.65	0.85	13.0	<5.	3.20	0.76
72701 B	17.1	44.0	27	8.26	1.32	1.69	6.08	0.849	6.36	0.79	14.5	5.3	2.94	0.73
73131 A	14.4	37.9	22	6.76	1.18	1.30	5.01	0.691	5.34	0.65	4.2	2.3	2.50	0.76
73131 B	15.0	38.8	26	7.02	1.18	1.35	5.14	0.708	5.27	0.69	7.3	2.9	2.56	0.71
73151 A	16.8	44.6	28	8.01	1.31	1.59	5.99	0.818	6.26	0.76	9.6	4.3	2.80	0.79
73151 B	14.9	39.6	22	7.14	1.23	1.44	5.39	0.744	5.43	0.70	10.2	4.1	2.56	0.70
73211 A	40.5	106.	72	20.3	1.52	3.76	11.1	1.47	6.20	0.80	7.4	3.4	4.70	0.97
73211 B	17.2	45.4	29	8.31	1.33	1.62	6.29	0.864	7.27	0.87	8.5	2.1	3.15	0.69
74111	14.2	37.7	25	7.50	1.31	1.62	5.78	0.808	6.05	0.84	8.0	2.3	2.40	0.60
74220	5.94	18.1	17	6.71	1.79	1.48	4.31	0.590	5.79	1.00	<6.	<4.	0.42	0.13
74241 A	9.72	29.0	22	9.05	1.68	2.19	7.78	1.12	7.59	1.26	3.5	3.5	0.99	0.40
74241 B	9.93	29.5	24	8.72	1.55	2.10	7.52	1.09	7.21	1.19	4.	4.	1.24	0.26
74261	9.37	27.0	17	8.21	1.63	1.91	6.95	0.960	6.98	1.18	4.5	<6.	1.10	0.23
75061 A	6.40	21.0	20	8.24	1.64	2.11	7.94	1.12	7.37	1.40	<5.	<6.	0.50	0.3
75061 B	7.34	21.3	20	8.62	1.74	2.18	8.21	1.12	7.93	1.40	5.	<7..	0.65	<1.
75081 A	8.01	24.1	21	8.83	1.75	2.15	8.12	1.12	7.82	1.38	5.4	<6.	0.75	<1.
75081 B	7.91	24.2	23	8.73	1.70	2.17	7.95	1.10	7.64	1.34	6.	<7.	0.81	<0.8
75111	8.96	26.2	20	7.56	1.56	1.71	5.98	0.860	6.17	1.01	6.	2.1	1.20	0.29
75121	9.07	26.6	17	7.84	1.59	1.82	6.41	0.922	6.65	1.06	12.	4.5	1.10	0.53
76031 A	8.91	25.2	16	5.78	1.25	1.37	4.81	0.667	4.78	0.73	32.	15.	1.45	0.33
76031 B	9.08	24.6	16	5.96	1.33	1.39	4.88	0.686	5.01	0.75	10.5	5.1	1.43	0.45
76121	8.66	24.8	18	6.92	1.46	1.62	5.71	0.825	5.86	0.93	7.	<5.	1.11	0.25
76131	11.8	32.3	23	7.17	1.41	1.61	5.70	0.802	5.53	0.86	7.1	1.9	1.87	0.52
76221 A	9.34	25.8	18	5.86	1.30	1.34	4.81	0.677	4.65	0.72	12.3	5.3	1.50	0.38
76221 B	10.3	27.7	18	6.09	1.30	1.36	4.84	0.687	4.72	0.74	6.7	2.1	1.72	0.38
76241 A	10.4	28.2	22	6.24	1.37	1.41	5.07	0.707	5.07	0.74	7.8	4.6	1.77	0.50
76241 B	11.7	32.0	22	6.88	1.35	1.47	5.33	0.744	5.42	0.76	7.1	2.6	1.84	0.49
76261 A	11.4	30.2	20	6.58	1.40	1.46	5.22	0.732	5.26	0.79	10.	3.1	1.84	0.49
76261 B	11.1	29.9	20	6.63	1.34	1.44	5.21	0.724	5.07	0.75	5.5	2.8	1.73	0.44
76281 A	8.74	25.0	19	5.90	1.33	1.39	4.92	0.673	4.86	0.82	7.0	3.2	1.44	0.37
76281 B	9.25	25.7	20	6.24	1.36	1.40	5.09	0.704	4.99	0.73	7.1	2.2	1.42	0.43
76321 A	11.6	31.3	21	6.73	1.35	1.47	5.39	0.730	5.57	0.78	7.4	4.0	2.08	0.58
76321 B	11.6	31.6	24	6.74	1.37	1.50	5.42	0.741	5.31	0.81	8.0	3.9	1.84	0.57
76501 A	9.41	25.1	n.a.	5.60	1.29	1.39	4.66	0.670	4.75	0.79	6.4	<5.	1.30	0.36
76501 B	8.98	24.3	20	5.67	1.28	1.29	4.61	0.659	4.64	0.69	7.8	3.4	1.43	0.37
77511	10.1	27.2	20	6.44	1.33	1.46	5.21	0.739	5.24	0.77	7.	2.3	1.69	0.41
77531	9.99	27.6	17	6.51	1.37	1.54	5.40	0.757	5.42	0.87	8.5	9.4	1.45	0.42
78121	8.98	24.9	17	6.24	1.36	1.44	5.14	0.751	5.31	0.79	10.5	2.5	1.32	0.32
78221 A	8.64	23.2	n.a.	5.83	1.31	1.35	4.74	0.680	4.89	0.76	8.2	<5.	1.10	0.22
78221 B	9.01	25.4	21	6.06	1.34	1.40	5.11	0.693	4.97	0.76	11.5	3.	1.30	0.34
78231	9.09	24.8	14	6.04	1.33	1.32	4.95	0.720	4.79	0.81	9.5	2.8	1.37	0.30
78250	8.81	25.0	18	6.30	1.36	1.51	5.41	0.726	5.38	0.74	9.5	4.	1.46	0.35
78421 A	7.92	21.9	16	5.69	1.31	1.43	4.94	0.699	5.13	0.80	9.5	3.0	1.25	0.35
78421 B	8.43	24.1	21	5.93	1.36	1.36	5.20	0.714	5.45	0.80	10.3	5.4	1.20	0.34
78441	9.09	24.9	18	6.29	1.36	1.38	5.14	0.737	5.07	0.72	9.0	3.5	1.40	0.35
78461	8.93	25.9	18	6.24	1.33	1.41	5.15	0.734	4.78	0.80	9.5	4.4	1.34	0.45
78481	9.03	24.8	23	6.20	1.37	1.44	5.24	0.715	5.07	0.82	13.	3.5	1.46	0.29
78501	8.44	23.7	16	6.67	1.38	1.61	5.65	0.796	5.91	0.91	<6.	n.a.	1.26	0.41
79121	8.79	26.1	20	7.44	1.56	1.81	6.32	0.875	6.01	1.06	8.	4.0	1.07	0.26
79221	8.21	23.5	20	7.02	1.49	1.79	9.32	1.46	45.7	0.99	7.5	5.	1.23	0.65
79241	9.45	27.2	21	7.55	1.58	1.72	6.30	0.877	6.19	0.98	10.	5.	1.36	0.40
79261	8.44	23.3	16	6.82	1.46	1.70	6.09	0.846	5.98	1.11	6.5	2.5	1.01	0.29
79511	8.51	26.1	18	7.49	1.58	1.80	6.26	0.885	6.00	0.99	9.	<5.	1.10	0.40
±	0.10	0.7	5	0.10	0.04	0.05	0.10	0.016	0.15	0.07	2.	2.	0.06	0.10

Designations "A" and "B" after sample numbers indicate that duplicate splits were analyzed. Uncertainties (±) are 1σ estimates of typical analytical precision. n.a. = not analyzed.

TABLE A2. Results of FB-EMPA, with 95% confidence limits (±) based on three probe spots per bead (values in percent oxide).

Sample	Station	SiO_2	TiO_2	Al_2O_3	FeO FB	FeO INAA	MgO	CaO
70181	AL	41.2	8.1	11.8	16.5		9.81	11.0
70271	SEP	40.6	8.4	12.6	16.1		9.38	11.3
70311	LRV-12	39.6	10.2	10.9	17.6		9.34	10.8
70321	LRV-12	40.2	9.8	11.4	17.1		9.38	10.6
71041	1	40.1	9.5	10.8	17.7		9.61	10.8
71131	1	39.9	10.0	10.6	17.5	17.9	9.58	10.8
71151	1	40.1	9.5	11.1	17.5		9.39	10.8
71501	1	39.6	10.0	10.8	17.6		9.77	10.8
72131	LRV-1	41.3	7.9	12.6	16.1		9.41	11.2
72150	LRV-3	42.2	5.7	14.5	14.5		10.26	11.3
72161	LRV-3	42.4	5.4	14.3	14.6		10.64	11.2
72241 B	2	45.3	1.33	21.0	8.79	8.59	9.63	12.5
72431 B	2	45.0	1.43	20.8	8.79	8.55	9.69	12.7
72701	2	44.9	1.56	20.7	8.60		9.85	12.9
73131 A	2A (RB)	45.0	0.81	22.9	7.16	6.87	9.13	13.5
73131 B	2A (RB)	45.0	1.03	22.2	7.31	7.18	9.58	13.4
73151 A	2A	44.9	1.30	21.4	8.45	8.60	9.61	12.8
73211 B	3	44.6	1.76	20.7	8.81	8.68	9.91	12.7
74111	LRV-5	44.8	2.6	19.9	9.59		8.91	12.7
74220	4	38.3	8.8	6.8	22.4	22.4	14.28	7.8
74241 A	4	40.8	8.7	12.9	16.2	16.2	8.80	11.1
74241 B	4	41.3	7.6	13.8	15.4	15.3	9.02	11.4
74242	4 (RGP)	44.5	2.8	20.0	9.65	9.73	9.24	12.3
74261	4	41.3	7.5	13.0	15.8		9.68	11.1
75111	LRV-7	41.8	6.8	12.8	16.0		10.25	10.7
75121	LRV-8	41.9	6.6	13.4	15.4		9.86	11.3
76031 B	6	43.0	3.4	18.7	10.7	10.9	10.40	12.2
76121	LRV-9	42.2	6.1	14.3	14.7		9.83	11.3
76131	LRV-10	43.5	3.7	17.5	11.0		10.51	12.1
76501 B	6	43.3	3.3	18.2	10.3		11.17	12.1
77511	7	44.0	3.8	17.4	11.4		9.99	11.9
77531	7	43.7	4.0	17.1	11.7		10.16	11.8
78121	LRV-11	43.2	4.5	16.3	12.6		10.02	11.9
78221 B	8	43.9	3.6	17.4	11.3		10.40	11.8
78231	8	43.6	4.1	16.5	12.2		10.38	11.7
78441	8	43.6	4.1	17.0	11.9		10.00	11.9
78501	8	42.8	5.2	15.6	13.1	13.4	10.05	11.7
79121	9	42.2	6.3	13.7	14.9		10.10	11.2
79221	9	41.9	6.3	13.8	15.1		10.04	11.3
79511	9	42.3	6.2	13.7	15.0		9.97	11.2
±		0.5	0.2	0.3	0.4		0.17	0.2

For samples with FeO values by INAA, fused beads were made from the INAA split after radioassay. Designations A and B refer to INAA subsplit of Table A1. RGP = ropy glass particles from 74242.

Acknowledgments. This work was supported by the National Aeronautics and Space Administration through grant NAG 9-56 to L. A. Haskin. We appreciate the assistance of B. L. Jolliff and A. M. Steele during sample analysis. The reviews of A. Basu, C. R. Neal, and an anonymous reviewer led to substantial improvements in the paper.

REFERENCES

Anders E. and Grevesse N. (1989) Abundances of the elements: Meteoritic and solar. *Geochim. Cosmochim. Acta, 53,* 197-214.

Arvidson R., Drozd R., Guiness E., Hohenberg C., Morgan C., Morrison R., and Oberbeck V. (1976) Cosmic ray exposure ages of Apollo 17 samples and the age of Tycho. *Proc. Lunar Sci. Conf. 7th,* pp. 2817-2832.

Baedecker P. A., Chou C.-L., Sundberg L. L., and Wasson J. T. (1974) Volatile and siderophile trace elements in the soils and rocks of Taurus-Littrow. *Proc. Lunar Sci. Conf. 5th,* pp. 1625-1643.

Bence A. E. and Albee A. L. (1968) Empirical correction factors for electron microanalysis of silicates and oxides. *J. Geol., 76,* 382-403.

Blanchard D. P., Haskin L. A., Jacobs J. W., Brannon J. C., and Korotev R. L. (1975) Major and trace element chemistry of boulder 1 at station 2, Apollo 17. *Moon, 14,* 359-371.

Boynton W. V., Baedecker P. A., Chou C.-L., Robinson K. L., and Wasson J. T. (1975) Mixing and transport of lunar surface materials: Evidence obtained by the determination of lithophile, siderophile, and volatile elements. *Proc. Lunar Sci. Conf. 6th,* pp. 2241-2259.

Brown R. W. (1977) A sample fusion technique for whole rock analysis with the electron microprobe. *Geochim. Cosmochim. Acta, 41,* 435-438.

Cavarretta G., Coradini A., Funiciello R., Fulchignoni M., Taddeucci A., and Trigila R. (1972) Glassy particles in Apollo 14 soil 14163,88: Peculiarities and genetic considerations. *Proc. Lunar Sci. Conf. 3rd,* pp. 1085-1094.

Crozaz G., Drozd R., Hohenberg C., Morgan C., Ralston C., Walker R., and Yuhas D. (1974) Lunar surface dynamics: Some general conclusions and new results from Apollo 16 and 17. *Proc. Lunar Sci. Conf. 5th,* pp. 2475-2499.

Duncan A. R., Erlank A. J., Willis J. P., Sher M. K., and Ahrens L. H. (1974) Trace element evidence for a two-stage origin of some titaniferous mare basalts. *Proc. Lunar Sci. Conf. 5th,* pp. 1147-1157.

Dymek R. F., Albee A. L., and Chodos A. A. (1975) Comparative petrology of lunar cumulate rocks of possible primary origin: Dunite 72415, troctolite 76535, norite 78235, and anorthosite 62237. *Proc. Lunar Sci. Conf. 6th,* pp. 301-341.

Fruland R. M., Morris R. V., McKay D. S., and Clanton U. S. (1977) Apollo 17 ropy glasses. *Proc. Lunar Sci. Conf. 8th,* pp. 3095-3111.

Goldstein J. I., Hewins R. H., and Axon H. J. (1974) Metal silicate relationships in Apollo 17 soils. *Proc. Lunar Sci. Conf. 5th,* pp. 653-671.

Haskin L. A., Shih C.-Y., Bansal B. M., Rhodes J. M., Wiesmann H., and Nyquist L. E. (1974) Chemical evidence for the origin of 76535 as a cumulate. *Proc. Lunar Sci. Conf. 5th,* pp. 1213-1225.

Heiken G. and McKay D. S. (1974) Petrography of Apollo 17 soils. *Proc. Lunar Sci. Conf. 5th,* pp. 843-860.

Heiken G. H., McKay D. S., and Brown R. W. (1974) Lunar deposits of possible pyroclastic origin. *Geochim. Cosmochim. Acta, 38,* 1703-1718.

Hunecke J. C., Jessberger E. K., Podosek F. A., and Wasserburg G. J. (1973) $^{40}Ar/^{39}Ar$ measurements in Apollo 16 and 17 samples and the chronology of metamorphic and volcanic activity in the Taurus-Littrow area. *Proc. Lunar Sci. Conf. 4th,* pp. 1725-1756.

Husain L. and Schaeffer O. A. (1973) Lunar volcanism: Age of the glass in the Apollo 17 orange soil. *Science, 180,* 1358-1360.

Jolliff B. L. (1991) Fragments of quartz monzodiorite and felsite in Apollo 14 soil particles. *Proc. Lunar Planet. Sci. Conf., Vol. 21,* pp. 101-118.

Korotev R. L. (1976) Geochemistry of grain size fractions of soils from the Taurus-Littrow valley floor. *Proc. Lunar Sci. Conf. 7th,* pp. 695-726.

Korotev R. L. (1981) Compositional trends in Apollo 16 soils. *Proc. Lunar Planet. Sci. 12B,* pp. 577-605.

Korotev R. L. (1987a) The nature of the meteoritic components of Apollo 16 soil, as inferred from correlations of iron, cobalt, iridium, and gold with nickel. *Proc. Lunar Planet. Sci. Conf. 17th,* in *J. Geophys. Res., 92,* E447-E461.

Korotev R. L. (1987b) The meteoritic component of Apollo 16 noritic impact melt breccias. *Proc. Lunar Planet. Sci. Conf. 17th,* in *J. Geophys. Res., 92,* E491-E512.

Korotev R. L. (1987c) Mixing levels, the Apennine Front soil component, and compositional trends in the Apollo 15 soils. *Proc. Lunar Planet. Sci. Conf. 17th,* in *J. Geophys. Res., 92,* E411-E431.

Korotev R. L. (1991) Geochemical stratigraphy of two regolith cores from the Central Highlands of the Moon. *Proc. Lunar Planet. Sci. Conf., Vol. 21,* pp. 229-289.

Laul J. C. and Papike J. J. (1980) The Apollo 17 drill core: Chemistry of size fractions and the nature of the fused soil component. *Proc. Lunar Planet. Sci. Conf. 11th,* pp. 1395-1413.

Laul J. C., Hill D. W., and Schmitt R. A. (1974) Chemical studies of Apollo 16 and 17 samples. *Proc. Lunar Sci. Conf. 5th,* pp. 1047-1066.

Laul J. C., Lepel E. A., Vaniman D. T., and Papike J. J. (1979) The Apollo 17 drill core: Chemical systematics of grain-size fractions. *Proc. Lunar Planet. Sci. Conf. 10th,* pp. 1269-1298.

Laul J. C., Papike J. J., and Simon S. B. (1981) The lunar regolith: Comparative studies of the Apollo and Luna sites. Chemistry of soils from Apollo 17, Luna 16, 20, and 24. *Proc. Lunar Planet. Sci. 12B,* pp. 389-407.

Lindstrom M. M. and Lindstrom D. J. (1986) Lunar granulites and their precursor anorthositic norites of the early lunar crust. *Proc. Lunar Planet. Sci. Conf. 16th,* in *J. Geophys. Res., 91,* D263-D276.

Lindstrom M. M., Crozaz G., and Zinner E. (1985) REE in phosphates from lunar highlands cumulates: An ion probe study (abstract). In *Lunar and Planetary Science XVI,* pp. 493-494. Lunar and Planetary Institute, Houston.

Lindstrom M. M., Lindstrom D. J., Korotev R. L., and Haskin L. A. (1986) Lunar meteorite Yamato-791197: A polymict anorthositic norite breccia. *Proc. Tenth Symposium on Antarctic Meteorites, Mem. Natl. Inst. Polar Res., Spec. Issue 41,* pp. 58-75. National Institute of Polar Research, Tokyo.

Lucchitta B. K. (1977) Crater clusters and the light mantle at the Apollo 17 site—A result of secondary impact from Tycho. *Icarus, 30,* 80-96.

Marinenko R. B. (1982) *Standard Reference Materials: Preparation and Characterization of K-411 and K-412 Mineral Glasses for Microanalysis: SRM 470.* National Bureau of Standards Special Publication 260-74, U.S. Govt. Printing Office, Washington.

McKay D. S., Morrison D. A., Clanton U. S., Ladle G. H., and Lindsay J. F. (1971) Apollo 12 soil and breccia. *Proc. Lunar Sci. Conf. 2nd,* pp. 755-773.

McKay D. S., Fruland R. M., and Heiken G. H. (1974) Grain size evolution of lunar soils. *Proc. Lunar Sci. Conf. 5th,* pp. 887-906.

McKay D. S., Bogard D. D., Morris R. V., Korotev R. L., Johnson P., and Wentworth S. J. (1986) Apollo 16 regolith breccias: Characterization and evidence for early formation in the mega-regolith. *Proc. Lunar Planet. Sci. Conf. 16th,* in *J. Geophys. Res., 91,* D277-D303.

Meyer C. Jr., Brett R., Hubbard N. J., Morrison D. A., McKay D. S., Aitken F. K., Takeda H., and Schonfeld E. (1971) Mineralogy, chemistry, and origin of the KREEP component in soil samples from the Ocean of Storms. *Proc. Lunar Sci. Conf. 2nd,* pp. 393-411.

Meyer C. Jr., McKay D. S., Anderson D. H., and Butler P. Jr. (1975) The source of sublimates on the Apollo 15 green glass and Apollo 17 orange glass spherules. *Proc. Lunar Sci. Conf. 6th,* pp. 1673-1699.

Meyer C., Galindo C., and Yang V. (1991) Lunar zircon (abstract). In *Lunar and Planetary Science XXII,* pp. 895-896. Lunar and Planetary Institute, Houston.

Morris R. V., Korotev R. L., and Lauer H. V. Jr. (1989) Maturity and geochemistry of the Van Serg core (79001/2) with implications for the micrometeorite component. *Proc. Lunar Planet. Sci. Conf. 19th,* pp. 269-284.

Morris R. V., Score R., and Dardano C. (1983) *Handbook of Lunar Soils.* JSC Publ. No. 19069, NASA Johnson Space Center, Houston. 914 pp.

Ostertag R., Stöffler D., Bischoff A., Palme H., Schultz L., Spettel B., Weber H., Weckwerth G., and Wänke H. (1986) Lunar meteorite Yamato-791197: Petrography, shock history and chemical composition. *Proc. Tenth Symposium on Antarctic Meteorites, Mem. Natl. Inst. Polar Res., Spec. Issue. 41,* 17-44. National Institute of Polar Research, Tokyo.

Rhodes J. M. (1977) Some compositional aspects of lunar regolith evolution. *Philos. Trans. R. Soc. London, A285,* 293-301.

Rhodes J. M., Rodgers K. V., Shih C., Bansal B. M., Nyquist L. E., Wiesmann H., and Hubbard N. J. (1974) The relationships between geology and soil chemistry at the Apollo 17 landing site. *Proc. Lunar Sci. Conf. 5th,* pp. 1097-1117.

Rhodes J. M., Hubbard N. J., Wiesmann H., Rodgers K. V., Brannon J. C., and Bansal B. M. (1976) Chemistry, classification, and petrogenesis of Apollo 17 mare basalts. *Proc. Lunar Sci. Conf. 7th,* pp. 1467-1489.

Rose H. J. Jr., Cuttitta F., Berman S., Brown F. W., Carron M. K., Christian R. P., Dwornik E. J., and Greenland L. P. (1974) Chemical composition of rocks and soils at Taurus-Littrow. *Proc. Lunar Sci. Conf. 5th,* pp. 1119-1133.

Ryder G. (1990) A distinct variant of high-titanium mare basalt from the Van Serg core, Apollo 17 landing site. *Meteoritics, 25,* 249-258.

Salpas P. A., Taylor L. A., and Lindstrom M. M. (1987) Apollo 17 KREEPy basalts: Evidence for nonuniformity of KREEP. *Proc. Lunar Planet. Sci. Conf. 17th,* in *J. Geophys. Res., 92,* E340-E348.

Salpas P. A., Lindstrom M. M., and Taylor L. A. (1988) Highland material at Apollo 17: Contributions from 72275. *Proc. Lunar Planet. Sci. Conf. 18th,* pp. 11-19.

Spudis P. D. and Ryder G. (1981) Apollo 17 impact melts and their relation to the Serenitatis basin. In *Multi-ring Basins, Proc. Lunar Planet Sci. 12A* (P. H. Schultz and R. B. Merrill, eds.), pp. 133-148. Pergamon, New York.

Stöffler D., Knöll H.-D., Marvin U. B., Simonds C. H., and Warren P. H. (1980) Recommended classification and nomenclature of lunar highlands rocks—A committee report. In *Proc. Conf. Lunar Highlands Crust* (J. J. Papike and R. B. Merrill, eds), pp. 51-70. Pergamon, New York.

Taylor G. J., Keil K., and Warner R. D. (1977) Very low-Ti mare basalts. *Geophys. Res. Lett., 4,* 207-210.

Vaniman D. T. and Papike J. J. (1977a) Very low Ti (VLT) basalts: A new mare rock type from the Apollo 17 drill core. *Proc. Lunar Sci. Conf. 8th,* pp. 1443-1471.

Vaniman D. T. and Papike J. J. (1977b) The Apollo 17 drill core: Modal petrology and glass chemistry (sections 70007, 70008, and 70009). *Proc. Lunar Sci. Conf. 8th,* pp. 3161-3193.

Wänke H., Palme H., Baddenhausen H., Dreibus G., Jagoutz E., Kruse H., Spettel B., Teschke F., and Thacker R. (1974) Chemistry of Apollo 16 and 17 samples: Bulk composition, late stage accumulation and early differentiation of the Moon. *Proc. Lunar Sci. Conf. 5th,* pp. 1307-1335.

Wänke H., Palme H., Baddenhausen H., Dreibus G., Jagoutz E., Kruse H., Palme C., Spettel B., Teschke F., and Thacker R. (1975) New data on the chemistry of lunar samples: Primary matter in the lunar highlands and the bulk composition of the Moon. *Proc. Lunar Sci. Conf. 6th,* pp. 1313-1340.

Warner R. D., Taylor G. J., Conrad G. H., Northrop H. R., Barker S., Keil K., Ma M.-S., and Schmitt R. (1979) Apollo 17 high-Ti mare basalts: New bulk compositional data, magma types, and petrogenesis. *Proc. Lunar Planet. Sci. Conf. 10th,* pp. 225-247.

Warren P. H. (1989) KREEP: Major-element diversity, trace-element uniformity (almost) (abstract). In *Workshop on Moon in Transition: Apollo 14, KREEP, and Evolved Lunar Rocks* (G. J. Taylor and P. H. Warren, eds.), pp. 149-153. LPI Tech. Rpt. 89-03, Lunar and Planetary Institute, Houston.

Warren P. H. and Kallemeyn G. W. (1986) Geochemistry of lunar meteorite Yamato-791197: Comparison with ALHA81005 and other lunar samples. *Proc. Tenth Symposium on Antarctic Meteorites, Mem. Natl. Inst. Polar Res., Spec. Issue 41,* 3-16. National Institute of Polar Research, Tokyo.

Warren P. H. and Wasson J. T. (1978) Compositional-petrographic investigation of pristine nonmare rocks. *Proc. Lunar Planet. Sci. Conf. 9th,* pp. 185-217.

Warren P. H. and Wasson J. T. (1979) The compositional-petrographic search for pristine nonmare rocks; Third foray. *Proc. Lunar Planet. Sci. Conf. 10th,* pp. 583-610.

Warren P. H., Jerde E. A., and Kallemeyn G. W. (1991) Pristine Moon rocks: Apollo 17 anorthosites. *Proc. Lunar Planet. Sci. Conf., Vol 21,* pp. 51-61.

Wentworth S., Taylor G. J., Warner R. D., Keil K., Ma M.-S., and Schmitt R. A. (1979) The unique nature of Apollo 17 VLT basalts. *Proc. Lunar Planet. Sci. Conf. 10th,* pp. 207-223.

Winzer S. R., Nava D. F., Lum R. K. L., Schuhmann S., Schuhmann P., and Philpotts J. A. (1975) Origin if 78235, a lunar norite cumulate. *Proc. Lunar Sci. Conf. 6th,* pp. 1219-1229.

Wolfe E. W., Bailey N. G., Lucchitta B. K., Muehlberger W. R., Scott D. H., Sutton R. L., and Wilshire H. G. (1981) *The Geologic Investigation of the Taurus-Littrow Valley: The Apollo 17 Landing Site* (R. M. Batson, K. B. Larson, and R. L. Tyner, eds.). U.S. Geol. Surv. Prof. Paper 1080.